Extent of QTL Reuse During Repeated Phenotypic Divergence of Sympatric Threespine Stickleback

Gina L. Conte,*,[1] Matthew E. Arnegard,*,[†] Jacob Best,* Yingguang Frank Chan,[‡,2] Felicity C. Jones,[‡,2] David M. Kingsley,[‡] Dolph Schluter,*,[3] and Catherine L. Peichel[†,3]

*Biodiversity Research Centre and Zoology Department, University of British Columbia, Vancouver, BC, Canada V6T 1Z4, [†]Divisions of Human Biology and Basic Sciences, Fred Hutchinson Cancer Research Center, Seattle, Washington 98109-1024, and [‡]Department of Developmental Biology and Howard Hughes Medical Institute, Stanford University School of Medicine, Stanford, California 94305-5329

ORCID ID: 0000-0003-0215-0777 (G.L.C.)

ABSTRACT How predictable is the genetic basis of phenotypic adaptation? Answering this question begins by estimating the repeatability of adaptation at the genetic level. Here, we provide a comprehensive estimate of the repeatability of the genetic basis of adaptive phenotypic evolution in a natural system. We used quantitative trait locus (QTL) mapping to discover genomic regions controlling a large number of morphological traits that have diverged in parallel between pairs of threespine stickleback (*Gasterosteus aculeatus* species complex) in Paxton and Priest lakes, British Columbia. We found that nearly half of QTL affected the same traits in the same direction in both species pairs. Another 40% influenced a parallel phenotypic trait in one lake but not the other. The remaining 10% of QTL had phenotypic effects in opposite directions in the two species pairs. Similarity in the proportional contributions of all QTL to parallel trait differences was about 0.4. Surprisingly, QTL reuse was unrelated to phenotypic effect size. Our results indicate that repeated use of the same genomic regions is a pervasive feature of parallel phenotypic adaptation, at least in sticklebacks. Identifying the causes of this pattern would aid prediction of the genetic basis of phenotypic evolution.

KEYWORDS genetics of adaptation; genetic parallelism; parallel evolution; repeated evolution; QTL mapping

We still have a poor understanding of the predictability of the genetic basis of phenotypic adaptation (Stern and Orgogozo 2008; Conte *et al.* 2012; Martin and Orgogozo 2013; Stern 2013). One way to make progress is to quantify the repeatability of the genetic changes that underlie repeated phenotypic evolution. When organisms independently evolve similar phenotypes in response to similar selection pressures (a reliable signature of adaptive evolution (Endler 1986; Harvey and Pagel 1991; Schluter 2000; Losos 2011), we can ask: How similar are the genetic "solutions" underlying those phenotypes? Many features may influence similarity of genetic solutions, including availability of standing genetic variation, mutational biases, and functional constraints. The extent to which the genetic basis of repeatedly evolved phenotypes is shared indicates the extent to which the genetic basis of adaptation is predictable.

Although there is some evidence indicating that gene reuse during repeated phenotypic evolution is common, current estimates of the frequency of gene reuse in adaptive evolution might not be accurate because of methodological limitations. A recent metaanalysis of studies of natural populations estimated that the average probability of gene reuse is 0.32–0.55 (depending on the type of data used to calculate it) across a diversity of taxa spanning divergence times from hundreds of years to hundreds of millions of years (Conte *et al.* 2012). The probability of gene reuse was highest among closely related species and it declined with increasing divergence time between the taxa being compared. This estimate of gene reuse was based on published cases in which a repeatedly evolved phenotype had either been genetically mapped in multiple populations or in which the role of a specific candidate gene on a given trait had been tested in different populations

doi: 10.1534/genetics.115.182550
Manuscript received June 24, 2015; accepted for publication September 10, 2015; published Early Online September 16, 2015.
Supporting information is available online at www.genetics.org/lookup/suppl/doi:10.1534/genetics.115.182550/-/DC1.
[1]Corresponding author: Biodiversity Research Centre, Department of Botany and Department of Zoology, 6270 University Blvd., Vancouver, British Columbia, Canada V6T 1Z4. E-mail: conte@zoology.ubc.ca
[2]Present address: Friedrich Miescher Laboratory of the Max Planck Society, Tübingen, 72076, Germany.
[3]These authors contributed equally to this work.

(Conte *et al.* 2012). However, caution is warranted when interpreting estimates based on both approaches. Candidate gene studies of repeated phenotypic evolution are prone to publication bias and have focused mainly on a small number of genes with mostly unknown effect sizes. Mapping studies of repeated phenotypic evolution have tended to focus on a small number of traits controlled by genes of apparently large effect. Few studies to date have mapped the genetic basis of a large number of repeatedly evolved phenotypes to quantitatively estimate the repeated use of the same loci.

To help remedy this gap, we investigated the genetic basis of repeated evolution in a large number of traits in two sympatric species pairs of threespine stickleback (*Gasterosteus aculeatus* species complex) from two isolated lakes in British Columbia, Canada. Both species pairs consist of a limnetic ecotype that specializes on zooplankton in the open water zone of the lake and a benthic ecotype that feeds on invertebrates from the littoral and benthic zones of the lake (McPhail 1984, 1992, 1994; Schluter and McPhail 1992). The species pairs appear to have originated independently in the past 10,000–12,000 years, following double invasions by ancestral marine populations into postglacial lakes (Schluter and McPhail 1992; McPhail 1994; Taylor and McPhail 2000; Jones *et al.* 2012a). Phenotypic divergence between species within each pair has occurred largely in parallel among the replicate pairs [that is, the phenotypes evolved in the same direction from a common ancestral species (Conte *et al.* 2012), and individuals of the same ecotype from different lakes strongly resemble one another (Schluter and McPhail 1992; Schluter and Nagel 1995; McKinnon and Rundle 2002; Gow *et al.* 2008)].

Here, we used a quantitative trait locus (QTL) approach to map many continuously varying, quantitative traits, as well as a few discrete traits that have diverged in parallel in the species pairs. This approach is a necessary first step in our effort to determine the frequency of gene reuse in this system because it provides the requisite locations of genetic factors underlying repeated phenotypic evolution, and the phenotypic effect sizes of these loci (Lynch and Walsh 1998; Broman and Sen 2009; Conte *et al.* 2012). Subsequent studies will address whether chromosomal regions that repeatedly underlie parallel phenotypic evolution in the two populations are due to mutations in at the same genes or different linked genes. However, our QTL results provide an interim estimate of gene reuse based on a large number of traits. We discuss the potential effects of this limitation on the interpretation of our results in *Discussion*.

In contrast to most previous studies, we used identical methods to simultaneously cross, raise, phenotype, and genotype fish, as well as to conduct linkage and QTL mapping. In both cases, we raised the F_2 hybrids in controlled, seminatural ponds, which allowed natural expression of the focal phenotypes. To measure QTL reuse, we implemented an Akaike information criterion (AIC) model selection approach to distinguish among alternative models of the effects of individual chromosomal regions on phenotypic divergence in the two species pairs. This allowed us to determine whether a QTL had parallel effects, an effect in one of the pairs but not the other, or effects in opposite directions in the two pairs. As a second measure of QTL reuse during parallel evolution, we calculated similarity between species pairs in the proportional contributions of QTL to trait differences, using the method of Conte *et al.* (2012). Finally, we tested whether the frequency of QTL reuse increases with their phenotypic effect sizes, as predicted by theory (Orr 2006).

Materials and Methods

Ethics statement

G.L.C. is certified by the Canadian Council on Animal Care (CCAC)/National Institutional Animal User Training (NIAUT) Program; certificate number 4061-11. Permission for collections of wild threespine sticklebacks used herein was granted by the following permits: British Columbia Ministry of the Environment permit numbers NA/SU08-42033 and NA/SU09-51805; Fisheries and Oceans Canada SARA permit number SECT 08 SCI 002 and SARA-116. Permission to care for and use threespine sticklebacks for the studies herein was granted by the University of British Columbia (UBC) Animal Care Certificate A07-0293 and the Fred Hutchinson Cancer Research Center Institutional Care and Use Committee protocol 1797.

Genetic crosses and experimental ponds

In 2009, we used wild-caught adult fish to make two *in vitro* interspecific crosses, one using fish from Paxton Lake and the other using fish from Priest Lake. Both crosses involved a limnetic female and a benthic male. We stored their bodies in 95% ethanol for DNA analysis. We reared the resulting F_1 hybrids in the laboratory. On May 2, 2010 we randomly selected 35 F_1 hybrid adults (19 female and 16 male) from the Paxton cross and 25 F_1 hybrid adults (12 female and 13 male) from the Priest cross. We took a sample of caudal fin tissue from each individual F_1 hybrid for DNA analysis and then released them into two separate experimental ponds (one for the Paxton cross and one for the Priest cross) at the UBC pond facility. These ponds (25 $\times$ 15 m surface area) were designed to harbor both benthic and limnetic habitat and contained a sloping shallow zone and a deep open-water zone (6 m deep) (Arnegard *et al.* 2014). To establish a natural prey base, we inoculated the ponds with macrophytes, sediments, and water full of aquatic insects, mollusks, and plankton from Paxton Lake. We did this once in the spring of 2009 (a year before releasing our F_1 hybrids) and once in the spring of 2011. We additionally added 1.25 kg of a 25.5:1 mix of 50% pure KNO_3:KH_2PO_4 in the spring of 2009 and again in the spring of 2010. After release, the F_1 hybrids were allowed to mate freely with their full siblings in the ponds throughout the breeding season. The following year, on September 14, 2011, we collected 407 adult F_2 hybrids from the Paxton Lake cross and 324 adult F_2 hybrids from the Priest Lake cross.

We euthanized F_2 hybrids using buffered MS222 and then took a sample of caudal fin tissue from each individual F_2 for DNA analysis. Then, we fixed each F_2 hybrid body in 10% formalin for morphological measurements. During the same summer, we collected an additional 230 F_2 hybrids from the Paxton Lake cross and 92 F_2 hybrids from the Priest Lake cross for a separate study. These F_2 hybrids were not included in the QTL mapping stage of this study but were used to construct the linkage map.

Wild-caught benthic and limnetic samples

To enable us to determine whether or not our focal phenotypes diverged in parallel, we obtained high-quality photos of Alizarin-Red–stained, wild-caught benthic and limnetic specimens from Paxton and Priest lakes. From these collections, made in the spring of 2005 (Ingram *et al.* 2012), we used 25 benthics and 21 limnetics from Paxton Lake and 36 benthic and 22 limnetics from Priest Lake. Since the Priest limnetic sample contained no females, we supplemented the collection with 23 additional Alizarin-Red–stained wild-caught Priest limnetics (10 female) that were collected, stained, and photographed in 1999 by J. Gow.

Phenotype measurements

We stained the F_2 specimens with Alizarin Red, following the methods of Peichel *et al.* (2001) and then took high-resolution lateral photographs, with a ruler in each photograph for scale. All of the following steps were done separately for the wild-caught benthic and limnetic collection and for the F_2 hybrid collection. Using tpsDig (Rohlf 2010), we digitized and scaled 26 morphological landmarks (Supporting Information, Figure S1) on the photos of the specimens. Photos were analyzed in random order. We measured centroid size as the square root of the sum of squared distances of the 26 landmarks from their centroid. We then performed generalized Procrustes superimposition on the *x*- and *y*-coordinates of the scaled landmarks using the R package "shapes" (Dryden 2013), resulting in 52 landmark coordinates that we analyzed as distinct traits. To correct for specimen bending, we followed the approach of Albert *et al.* (2008).

We scored five skeletal meristic traits (*i.e.*, countable quantitative traits: number of lateral plates along the right side of the body; presence/absence of first and second dorsal spines; the number of long and short gill rakers on the first gill arch on the left side of the body) (Figure S1) using the fixed and stained F_2 specimens. In the absence of the wild-caught reference fish specimens, we scored meristic traits using their photos. However, since photos do not show the gill rakers, we could not count the long and short gill rakers on the first gill arch for the wild-caught benthic and limnetic samples, as was done for the F_2 hybrids. Instead we used counts taken by Ingram *et al.* (2012) of the total gill raker number on the first gill arch for the same individuals. For the 23 additional Priest limnetic fish, no gill raker counts were available, and thus, they were left out of the test of parallelism in gill raker divergence.

We tested for and removed significant outlier data points for all traits using the function "outlierTest" in the R package "car" (Fox *et al.* 2013). F_2 hybrids that were standard length outliers were dropped from the study (four Paxton individuals and one Priest individual).

Identifying parallel phenotypic evolution

We classified divergence in a trait as "parallel" when the ecotype difference in the trait was in the same direction in both lakes (*i.e.*, benthics had a higher mean than limnetics in both lakes, or vice versa), though not necessarily of the same magnitude. We classified divergence in a trait as "opposite" when the ecotype difference was in opposite directions in the two lakes (*i.e.*, benthics had a higher mean than limnetics in one lake and a lower mean than limnetics in the other). If the ecotypes differed in a trait in only one of the two lakes, we classified divergence in the trait as "single lake." Finally, if the species did not differ in a trait in either lake, we classified divergence in the trait as "neither lake." For each trait, we tested these scenarios by fitting five linear models to phenotypes of our wild-caught benthics and limnetics from both lakes and then deciding which fit the data best (Table S1). The models were as follows.

Model 1, "same effect," was a linear model that fitted the given trait to the explanatory variable ecotype (benthic *vs.* limnetic). Model 2, "different effect," included the ecotype variable and its interaction with lake (Paxton *vs.* Priest). Including the interaction allowed the detection of a difference between lakes in the magnitude and direction of the difference between the two ecotypes. In model 3, "effect in Paxton only," an explanatory variable was fitted that constrained the benthic and limnetic species of Priest Lake to the same mean, while allowing the means to differ in Paxton Lake. The reverse was done in model 4, "effect in Priest only." Finally in model 5, "no effect," the given trait was fitted to a constant, which constrained benthics and limnetics from both lakes to have the same mean. All five models included sex as a covariate.

We used the AICc value to determine the best model for each trait and then grouped the traits accordingly into the four divergence categories. Trait divergence was classified as parallel either if model 1 was the best or if model 2 was the best and the trait difference between the two ecotypes was in the same direction in the two lakes. Traits were classified as single lake if either model 3 or 4 was the best. Trait divergence was classified as opposite if model 2 was the best and the effect of species was in opposite directions in the two lakes. Finally, a trait was classified as divergent in neither lake if model 5 was the best.

For 15 traits, more than one trait divergence category fit the data nearly equally well. That is, the ΔAICc value between the best and second best models was <2 (Burnham and Anderson 2002) and the second best model represented a different trait divergence category than the best model (Table S1). These 15 traits were left out of all calculations and analyses in which trait divergence category was a variable. Finally,

because the gill raker counts for the wild-caught reference fish were of the total number on the first gill arch, rather than the subdivided counts of long and short rakers on the first arch, as was scored in our F_2 hybrids, the trait divergence category determined for the total number of gill rakers was inferred to be the trait divergence category of the subdivided counts as well. However, when calculating the proportion of traits in each trait divergence category (parallel, single lake, or opposite), only the total gill raker count was considered (therefore, $N = 57$ rather than $N = 58$ traits for those calculations).

Single nucleotide polymorphism genotyping

We isolated genomic DNA from caudal fin tissue of the 4 F_0 progenitors, 60 F_1 hybrids and 1057 F_2 hybrids (407 + 230 from the Paxton cross and 324 + 92 from the Priest cross) using either Proteinase K digestion, phenol-chloroform extraction, ethanol precipitation, and resuspension of the precipitated DNA in 30 μl of TE buffer (10 mM Tris, 1 mM EDTA, pH 8.0), or the DNeasy 96 Blood and Tissue Kit (Qiagen), using only 30 μl of buffer AE for the first elution. We then diluted an aliquot of each sample using TE buffer to a DNA concentration between 3 ng/μl and 150 ng/μl, based on the PicoGreen assay (Life Technologies).

We genotyped all F_0, F_1, and F_2 individuals using Illumina's GoldenGate assay and a custom multiplex oligonucleotide pool developed for a recently published collection of single nucleotide polymorphisms (SNPs) (Jones *et al.* 2012a). We found 430 of these SNPs to be polymorphic in at least one of our crosses (246 were polymorphic in the Paxton cross and 318 were polymorphic in the Priest cross, 134 of which were polymorphic in both). See Table S2 for the identities, genomic locations, and National Center for Biotechnology Information (NCBI) identification numbers for all 430 SNP markers. The Illumina Sentrix Array Matrices used for genotyping were processed at the Genomics Shared Resource of the Fred Hutchinson Cancer Research Center. We scored genotypes from the raw data using GenomeStudio software (Illumina).

Linkage mapping

We created a linkage map with JoinMap ver. 3.0 (Ooijen and Voorrips 2002), coding F_2 hybrid genotypes according to the "cross-pollinator" population code for outbred crosses between two diploid parents. To determine F_1 parentage of each F_2 hybrid, we used the R package "MasterBayes" (Hadfield 2013) to reconstruct pedigrees based on the full SNP dataset. When creating the linkage map, we only included $F_1 \times F_1$ families containing at least 10 F_2 hybrids. This included 268 F_2 hybrids from the Paxton cross and 261 F_2 hybrids from the Priest cross, some of which were not part of the QTL mapping study, as noted above.

To estimate a linkage map based on all families, we used JoinMap ver. 3.0 to compute all obtainable pairwise recombination fractions and associated base 10 logarithm of odds (LOD) scores between SNP markers for each $F_1 \times F_1$ family (hereafter "family") separately. We then combined the pairwise recombination fractions from the different families into a single data file and used JoinMap to produce a single combined Paxton–Priest linkage map. Using a similar procedure, we also created separate linkage maps for each lake. We detected all the same QTL in each lake whether we used the combined map or the separate map for that lake (data not shown). Therefore, we proceeded with the use of the combined map for the remaining analyses. Our combined linkage map had a total genetic length of 876.68 cM. It contained SNP markers every 2.15 cM on average, which translates to ~1.14 Mb of physical distance based on the reference stickleback genome assembly (Broad S1, February 2006) (Jones *et al.* 2012b).

Identifying candidate QTL

To identify a set of chromosomal regions at which to conduct tests of genetic parallelism, we carried out three QTL scans to identify those chromosomal regions that had a phenotypic effect on a given trait in at least one of the lakes. These we termed "candidate QTL." Only parallel phenotypic traits were used in these analyses. Each of the three scans involved interval mapping using Haley–Knott regression via the "scanone" function in R/qtl and included family identity and sex as covariates. We used F_2 genotype coding (Broman and Wu 2013), in which case scanone detects additive and/or dominance components of genotypes when testing for QTL. The first scan used only the F_2 hybrids from the Priest Lake cross ($N = 323$). The second scan used only the F_2 hybrids from the Paxton Lake cross ($N = 403$). The third scan used the F_2 hybrids from both crosses and included a genotype × cross interaction as a covariate. For simplicity, we grouped all F_2 hybrids from singleton families into a single pseudofamily. This pseudofamily consisted of 20 F_2 hybrids from the Priest Lake cross and 24 F_2 hybrids from the Paxton Lake cross. Results did not change when we coded F_2 hybrids from singleton families into their own family instead. For each trait, we performed 10,000 permutations to determine the genome-wide LOD thresholds for significant QTL at the $\alpha = 0.05$ and $\alpha = 0.01$ levels. We present detailed results below for the 0.05 level and then describe how they are modified when we use the 0.01 level instead. We did not employ more stringent thresholds to account for multiple traits because our goal was to determine the frequency of gene reuse on a per-trait basis with conventional significance levels.

Thirty-nine of 40 candidate QTL discovered in the combined scan were also detected in one or both of the single-lake scans, as indicated by overlapping 1.5 LOD confidence intervals. In this case, we used the QTL position from the combined scan as our candidate QTL as it offered a fixed position at which to test for parallelism. Ten additional candidate QTL were detected in the Paxton Lake scan and 8 were detected in the Priest Lake scan. All detected candidate QTL are shown in Table S3, Table S4, and Table S5.

Genetics of parallel evolution

We classified the effects of a QTL as parallel when its phenotypic effect was in the same direction in both lakes (*i.e.*, F_2 hybrids with two benthic alleles at the QTL had a higher mean than F_2 hybrids with two limnetic alleles in both lakes, or vice versa), though not necessarily of the same magnitude. We classified the effects of a QTL as opposite when its phenotypic effect was in opposite directions in the two lakes (*i.e.*, F_2 hybrids with benthic genotypes had a higher mean than F_2 hybrids with limnetic genotypes in one lake and the opposite in the other lake). If the phenotypic effect of a QTL was present in only one of the lakes, we classified the effect of the QTL as single lake. We tested these scenarios for each candidate QTL and corresponding trait, by fitting five linear models to the trait values of F_2 hybrids from both lakes combined, and then deciding which fit the data best (Table S6).

To fit the linear models, we first converted genotype information to additive and dominance scores, reflecting the additive and dominance components of genotype effects on the trait. The additive score varied between 0 and 1 and reflected the estimated proportion of the genotype inherited from the benthic grandparent. The additive score was calculated as $0.5 - P(\mathrm{AA})/2 + P(\mathrm{BB})/2$, where $P(\mathrm{AA})$ is the probability that the genotype at a chromosome position is homozygous limnetic, and $P(\mathrm{BB})$ is the probability it is homozygous benthic. The dominance score varied between 0 and 0.5 and reflects half the estimated probability that the genotype is heterozygous. The dominance score was calculated as $P(\mathrm{AB})/2$, where $P(\mathrm{AB})$ is the probability the genotype is a heterozygote. QTL effects were evaluated with linear models that included both additive and dominant genotype variables as main effects. Genotype probabilities were calculated using the R/qtl function "calc.genoprob" (Broman and Wu 2013).

In model 1, "same effect," we fitted the trait measurements with a linear model that included the additive and dominance effects of QTL genotype. Model 2, different effect included both the main effects of QTL genotype and the interaction between the additive score and lake. The presence of the interaction fits a different effect of the additive component in the two lakes. In model 3, "effect in Paxton only," the data were fitted to a modified genotype variable that allowed for differences in trait means between QTL genotypes in Paxton Lake but constrained different Priest Lake genotypes to have the same mean. The reverse was done in model 4, "effect in Priest only." Finally in model 5, "no effect," the effects of QTL genotype were dropped completely. All models included family and sex as covariates.

We then grouped the 58 candidate QTL into the three QTL effect categories based on which model had the lowest AICc value, which we term the "best model." QTL were classified as parallel if either model 1 was the best or model 2 was the best and the effect of the QTL was in the same direction in the two lakes. QTL were classified as single lake if either model 3 or 4 was the best. QTL were classified as opposite if model 2 was the best and the effect of the QTL was in opposite directions in the two lakes. Model 5 was never the best, so all QTL were accounted for by the first 4 models. For 15 of the candidate QTL, more than one QTL effect category fit the data nearly equally well, as judged by an AICc difference <2 (Table S6). These 15 candidate QTL were left out of all calculations and analyses in which QTL effect category was a variable.

QTL reuse and pleiotropy

The proportion of traits whose QTL are parallel may be a biased estimate of genetic parallelism if the underlying genetic changes are pleiotropic, affecting multiple traits. We carried out three additional procedures to minimize such bias. First, we inspected correlations between traits in the F_2 individuals to assess the extent to which traits vary independently (Figure S2 and Figure S3). Second, we conservatively treated all QTL on the same chromosome as though they represented a single QTL and measured parallelism between lakes as the proportion of traits mapping to that chromosome whose QTL had parallel, single lake, or opposite phenotypic effects. This procedure counts each chromosome and QTL only once when calculating the genome-wide average proportion of parallel QTL and eliminates bias if each chromosome indeed has just one causative gene. Third, we repeated our phenotypic and genetic model selection analyses on uncorrelated principal components of phenotypic variation in the F_2 hybrids rather than the original traits. Although the total number of principal components must equal the number of traits, any suite of traits affected by the same underlying pleiotropic gene or genes should covary in the F_2 hybrids. In this case, the majority of genetic variation in the F_2 hybrids will be captured by a reduced number of principal components that map to detectable QTL.

Our principal component analysis (PCA) was conducted on the 32 parallel phenotypic traits in F_2 individuals from Paxton and Priest lakes using the correlation matrix. Here we used total number of gill rakers rather than the subdivided counts. F_2 values were first corrected for mean differences between sexes and lakes. Only individuals with no missing phenotype data were included in the PCA (396 Paxton F_2 hybrids; 317 Priest F_2 hybrids). We first determined whether each of these 32 principal component phenotypes diverged in parallel in the pure-species fish from the two lakes using the model selection technique described above in the *Identifying parallel phenotypic evolution* subsection. To obtain the principal component phenotypes for pure-species fish, we corrected for differences between sexes and lakes as was done for F_2 hybrids, and we also corrected for differences between the means of pure-species and F_2 fish. We then projected the pure-species fish onto the F_2 principal components. Only individuals with no missing phenotype data were included in the PCA (30 Paxton individuals; 55 Priest individuals). For the 17 parallel principal components, we then obtained a set of 25 candidate QTL (Table S7) using the methods described in the *Identifying candidate QTL* subsection above. Finally, we used the model selection technique described in the *Genetics*

of parallel evolution subsection above to classify principal component QTL effects as parallel, single lake, or opposite. In a modification of this third approach, we also carried out the model selection analysis only on the first 18 principal components (rather than all 32), which cumulatively accounted for 89.3% of the phenotypic variation in the F_2 cross (Table S7). This approach should reduce bias by reducing redundancy caused by pleiotropy, and it also ignores QTL underlying principal components having little phenotypic variation in the F_2 hybrids.

Proportional similarity of QTL use

In a separate approach to measuring genetic parallelism, we estimated the proportional similarity of QTL use (Conte *et al.* 2012) underlying each trait represented in our candidate QTL dataset ($N = 26$ traits) by first fitting multiple QTL models to parallel phenotypic traits using the R/qtl function "fitqtl" (Broman and Wu 2013) (multiple QTL mapping, MQM; Table S8). We did this separately for the two lakes. We first retested each candidate QTL and its corresponding trait one at a time and dropped any QTL that were not significant at $\alpha = 0.05$. These models included family and sex as covariates. The effects of surviving QTL were then estimated by entering them into a multiple QTL model that included the main effects of those QTL genotypes, as well as family and sex as covariates. Nonsignificant QTL were assumed to have zero effect.

We calculated the proportional similarity of QTL use underlying each trait following the methods of Conte *et al.* (2012). For each lake separately, the percent of the phenotypic variance explained by QTL (PVE) of all QTL included in the multiple QTL model for a given trait were scaled so that their sum was equal to 1, resulting in proportional contributions of each QTL to the phenotype (Table S8). We then calculated proportional similarity as the overlap in the distribution of proportional contributions; $PS = \Sigma_i \min(p_{i1}, p_{i2})$, where p_{i1} and p_{i2} are the proportional contributions of QTL_i in the two lakes. Because this approach focuses on the extent to which the same loci are repeatedly involved, overlaps in the proportional contributions of loci are counted regardless of whether their phenotypic effects are in the same direction or not.

QTL reuse and effect size

To test the relationship between effect size and QTL reuse, first we extracted the largest effect QTL for a given phenotypic trait in each lake (traits without at least one QTL in both lakes were not considered). We used PVE as our measure of effect size. We then scored the trait according to whether the QTL was the same (occurred at the same genomic location) or different in the two lakes. This was repeated for every phenotypic trait that had diverged in parallel between the Priest and Paxton lake pairs (15 traits in total fit the criteria). We determined PVE for each candidate QTL in each lake separately by fitting each QTL to its corresponding trait in linear models as described above. These models included family and sex as covariates. We calculated PVE as the absolute value of the difference in the residual sum of squares explained by the full model and a reduced model from which the QTL was dropped divided by the total sum of squares explained by the full model. The PVEs of candidate QTL that were not significant at $\alpha = 0.05$ were assumed to be 0. For each parallel phenotypic trait that had at least one significant QTL in each lake, we then asked whether the largest effect QTL underlying that trait was the same in both lakes or not.

QTL reuse and genotype information

We tested whether genotype information explained any variation in QTL results. We used entropy to measure the proportion of missing genotype information, obtained using the function "plot.info" in R/qtl (Broman and Wu 2013) (Figure 1). Lower entropy indicates greater genotype information. Entropy was calculated directly for QTL occurring at SNP markers, and using interpolation when QTL occurred between two SNPs. We then asked whether single-lake QTL were associated with larger differences in entropy between the lakes than QTL with an effect in both lakes (parallel or opposite), using a Wilcoxon rank-sum test. Fifteen candidate QTL were left out of this analysis because more than one QTL effect category fit the data nearly equally well. The analysis included the remaining 43 candidate QTL underlying traits that evolved in parallel.

Data availability

File S1 contains phenotype data for all F_2 hybrids, all pure benthics and all pure limnetics from Paxton and Priest Lakes. File S2 contains all F_0, F_1 and F_2 SNP genotypes for all families in the Paxton Lake cross. File S3 contains all F_0, F_1 and F_2 SNP genotypes for all families in the Priest Lake cross.

Results

Parallel phenotypic evolution

We found that of 42 traits assigned to a divergence category, 32 (76.2%) diverged in parallel in the two pairs. Divergence in the other 10 traits was nonparallel, with 5 (11.9%) divergent in only a single pair and 5 divergent in opposite directions in the two pairs (Table S1). Thus, the majority of morphological traits diverged in parallel between the species pairs, though evolution in a substantial number of traits has been nonparallel. For the remainder of the study we focused on the genetic basis of the traits that diverged in parallel, thereby allowing us to estimate the repeatability of the genetics of adaptation.

Genetics of parallel evolution

We performed QTL mapping of the 33 phenotypic traits that diverged in parallel (33 traits rather than 32 due to separation of gill raker counts into long and short gill raker counts). We detected a total of 58 QTL that had an effect in one or both pairs underlying 26 of the 33 traits (Figure 1 and Figure 2; Table S3, Table S4, and Table S5). These 58 QTL represent

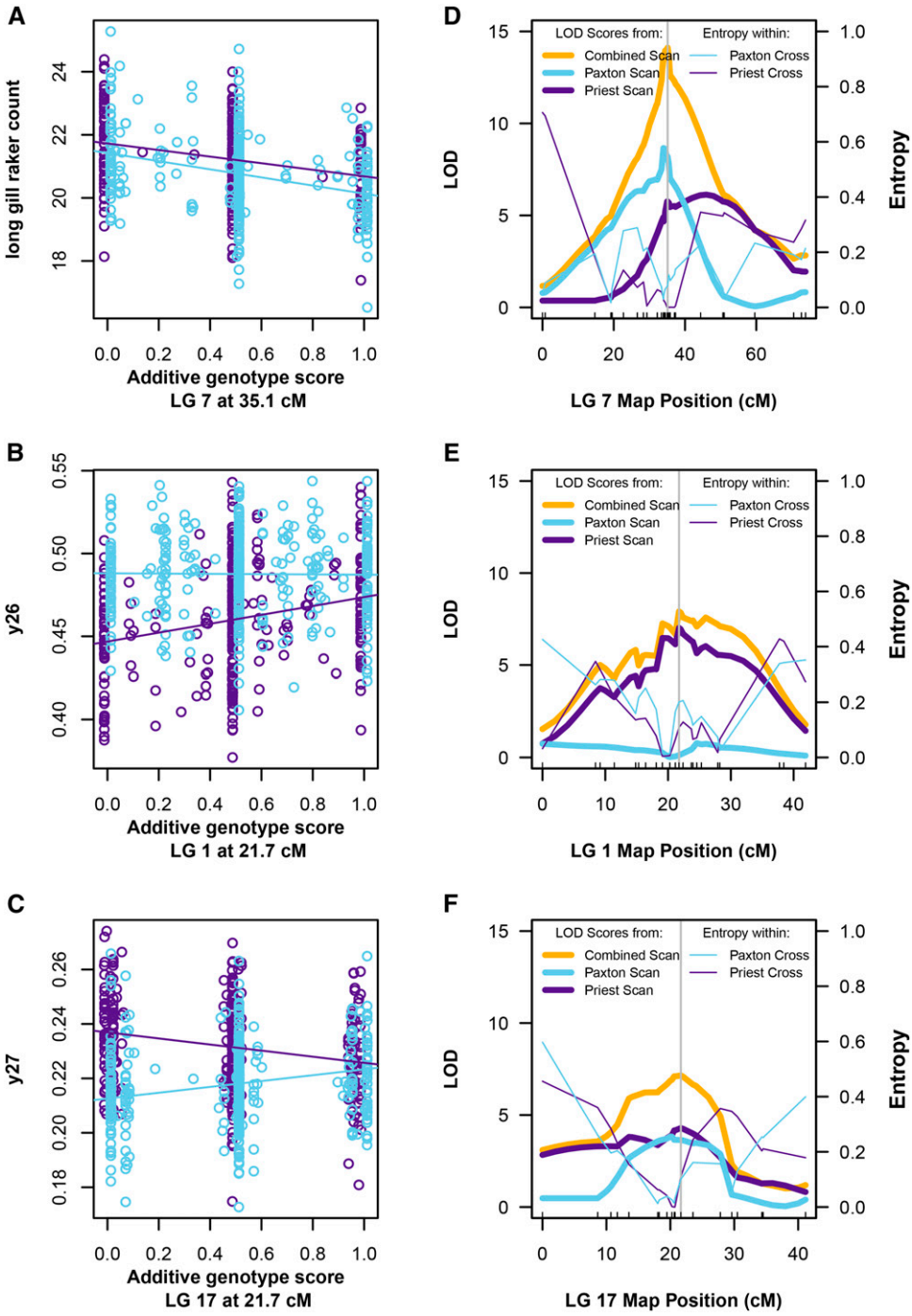

Figure 1 Examples of QTL with parallel, single-lake, and opposite effects. (A–C) F_2 phenotypes from the Paxton Lake cross (light blue) and the Priest Lake cross (purple) are shown on the vertical axes. Additive genotype scores at candidate QTL are shown on the horizontal axes, with 0 indicating two limnetic alleles, 1 indicating two benthic alleles, and 0.5 the heterozygote. Values in between these categories indicate uncertain genotypes (see *Materials and Methods*). Lines represent the fitted values of linear models fitted to the phenotype and genotype data for each lake (light blue, Paxton Lake cross; purple, Priest Lake cross). F_2 family identity and sex were covariates in fitted models. Phenotypic measurements shown here are corrected for family identity. (D–F) For the same three QTL (one QTL per row), the plots in the right column show the LOD profiles (left vertical axis and bold lines) from the three distinct QTL scans across the entire linkage group on which the QTL was detected (horizontal axis). They also show the entropy scores (an index of missing genotype information) for each lake's cross across the entire linkage group (right vertical axis and nonboldface lines). The positions of SNPs markers in the combined Paxton and Priest linkage map are depicted by tick marks. The vertical gray line represents the position of the peak marker in the combined scan (gold).

candidate chromosomal positions at which we subsequently tested for parallel QTL effects.

Figure 1 shows examples of classified QTL and traits illustrating the three model selection outcomes: parallel, single lake, and opposite. The number of long gill rakers in F_2 hybrids decreases with an increasing number of benthic alleles at a candidate QTL on linkage group (LG) 7 in parallel in both species pairs (Figure 1A). The trait "landmark y26" (the *y*-coordinate of a landmark placed on the dorsum of the trunk over the pectoral fin midpoint) increases with an increasing number of benthic alleles at a candidate QTL on LG 1 in Priest Lake but not in Paxton Lake (Figure 1B). The trait "landmark y27" (the *y*-coordinate of a landmark placed at the posterior insertion of the dorsal fin at the first soft ray) changes with the genotype at a candidate QTL on LG 17 in both pairs, but in opposite directions (Figure 1C).

Of the 43 candidate QTL classified into QTL effect categories, representing 23 parallel phenotypic traits, 21 (48.8%) had parallel effects in the two pairs (Figure 2; Table S6). That is, almost half of these QTL that underlie parallel phenotypic evolution had phenotypic effects in the same direction in crosses from both lakes, though not necessarily of identical

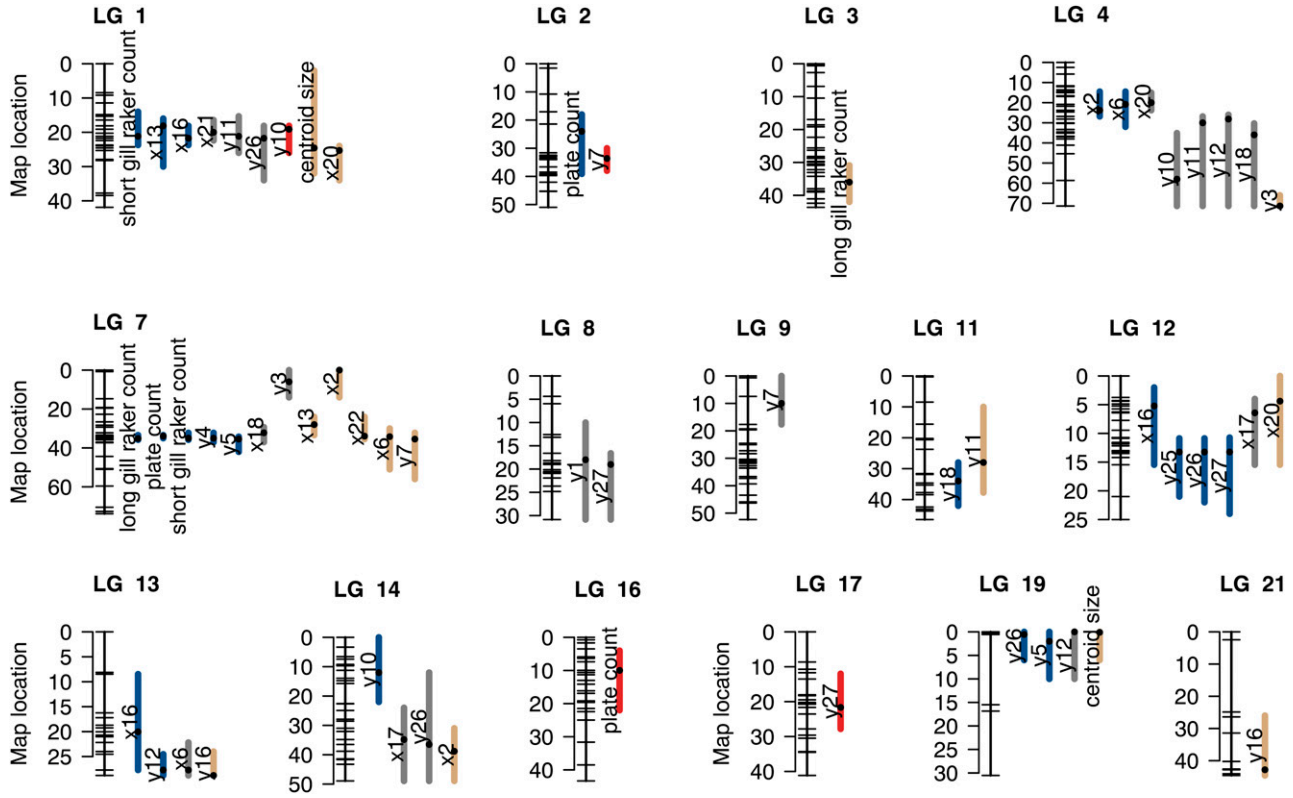

Figure 2 Map of candidate QTL. Map of 58 candidate QTL (*i.e.*, QTL with an effect in one or both lakes). Linkage groups on which QTL were detected are shown. For each, the positions of SNPs markers in the combined Paxton and Priest linkage map are depicted by tick marks on the left. Colored bars span the 1.5-LOD confidence intervals of candidate QTL. Black dots within bars represent the peak marker position. The phenotype affected by each candidate QTL is indicated to the left of its bar. Colors of bars represent the "QTL effect" category, as follows: parallel effects, blue; effect in only one lake, gray; and opposite effects, red. Tan colored bars represent the candidate QTL for which more than one QTL effect category fit the data nearly equally well.

magnitudes. A slightly smaller fraction (41.9%, $N = 18$) had an effect in one lake but not the other. Finally, a minority (9.3%, $N = 4$) had phenotypic effects in opposite directions in the two pairs (Figure 2; Table S6). Using a more stringent significance threshold of $\alpha = 0.01$ revealed similar proportions of QTL ($N = 18$) with parallel (67%; $N = 12$;), single lake (22%; $N = 4$), and opposite effects (11%; $N = 2$;), suggesting that the results are robust to significance threshold.

QTL reuse and pleiotropy

Many classified QTL were located in clusters on the same chromosomal regions (Figure 2). It is possible that multiple phenotypes map to the same locations because of the pleiotropic effects of a smaller number of loci. We carried out three checks to ensure that overcounting of QTL did not bias our results. First, we found that most, but not all, correlations between parallel traits in the F_2 hybrids were low (Figure S2 and Figure S3). Second, when we reduced the data to 13 QTL groups by combining all QTL on the same chromosome, we found that the average proportions of parallel, single lake, and opposite effects per chromosome were similar to the proportions based on the separate QTL (41.5% ± 9.6% SE parallel, 38.1% ± 10.1% SE single lake, and 20.3% ± 10.5% SE opposite effects; Figure S4). Third, we repeated our genetic analysis using uncorrelated principal components rather than the original traits. Of the 32 principal components, we mapped the 17 principal components that were found to be phenotypically parallel in the two lakes, which is fewer than the original number of parallel traits ($N = 32$). This analysis identified 25 candidate QTL, of which 16 could be classified using our model selection technique (Table S7). Of these, the majority had parallel effects (62.5%, $N = 10$), a minority had an effect in one lake but not the other (37.5%, $N = 6$), and no QTL had effects in opposite directions. Interestingly, we were able to identify QTL for principal components that explained relatively little of the phenotypic variance in the F_2 crosses (Table S7). However, in a modification of this procedure, we considered only the 18 principal components that accounted for the first 90% of cumulative phenotypic variance in F_2's. Of the 18, only 13 were phenotypically parallel and they mapped to 15 QTL that could be classified using model selection. The results were similar to the previous analysis: most QTL had parallel effects (66.7%, $N = 10$), a minority had single lake effects (33.3%, $N = 5$), and none had opposite effects (Figure S5). The similarity of the results of these varied approaches suggest that trait correlations caused by pleiotropy have not greatly biased the results based on single traits.

Proportional similarity of QTL use

Across the 26 traits that had undergone parallel phenotypic evolution, and for which QTL were detected (Table S8), average proportional similarity of QTL use was 0.38 ± 0.07 SE. Whereas the frequency of QTL with parallel effects reflects how commonly QTL have phenotypic effects in the same direction in both pairs, proportional similarity of QTL use measures the similarity of the full distribution of QTL effects of a trait in the two pairs (Conte *et al.* 2012).

QTL reuse and effect size

To test the relationship between effect size and parallelism of QTL effects, we asked whether the largest effect QTL was in the same or different genomic locations in the two pairs for each parallel phenotypic trait having at least one QTL in each pair ($N = 15$). We assumed that phenotypic effect sizes of QTL are positively correlated with fitness effect sizes (Orr 2006) and used PVE as our measure of effect size. We predicted that the two QTL should be the same QTL (occur at the same location) more often when their effects are both large than when their effects are both small. However, we found that the largest effect QTL for individual phenotypic traits were no more likely to be the same in both pairs when the mean of their effect sizes was relatively large than when the mean of their effect sizes was relatively small ($t = -0.69$, d.f. = 9.31, $P = 0.51$) (Figure 3). We did, however, observe a tantalizing trend, whereby the two traits with the largest-effect QTL in both pairs indeed mapped to the same genomic location (Figure 3).

QTL reuse and genotype information

We tested whether classification of QTL as single lake was associated with a difference between species pairs in genotype information, as measured using entropy, compared with QTL detected in both lakes (parallel or opposite) (Broman and Wu 2013). Genotype information may be lower in one pair than the other if, for example, a marker is informative in the grandparents of the cross from one lake but not the other, or if the frequency of missing genotypes at a marker differs between F_2 hybrids from the two crosses. This alone could cause differences in apparent QTL effects in the two lakes. We found that differences in the proportion of missing genotype information between the crosses were generally small (0–0.2), and there were no significant overall differences in missing genotype information between QTL detected in both pairs *vs.* in only one pair (Wilcoxon rank-sum test, $W = 293.5$, d.f. = 1, $P = 0.09$) (Figure 4). However, a few large entropy values occurred in the single-lake QTL category; such effects might have caused us to slightly overestimate the frequency of QTL in the single-lake category and underestimate the frequencies of QTL in the other two categories.

Discussion

We found that almost half of genomic regions underlying parallel phenotypic differences between the Paxton and Priest lake species pairs themselves had parallel effects. That is, in approximately half the cases, the phenotypic effects of QTL alleles inherited from a given ecotype were in the same direction in the crosses from both pairs. We also found that the average proportional similarity of QTL use underlying parallel phenotypic traits was 0.38 between the two pairs. Because our focal phenotypes have repeatedly evolved in correlation with the environment and are therefore likely to be adaptive (Endler 1986; Harvey and Pagel 1991; Schluter 2000; Losos 2011), these values estimate the repeatability of the QTL underlying parallel phenotypic adaptation. Our study is one of the first to use simultaneous mapping to measure the repeatability of the genetics of adaptation using a large number of parallel traits in wild species.

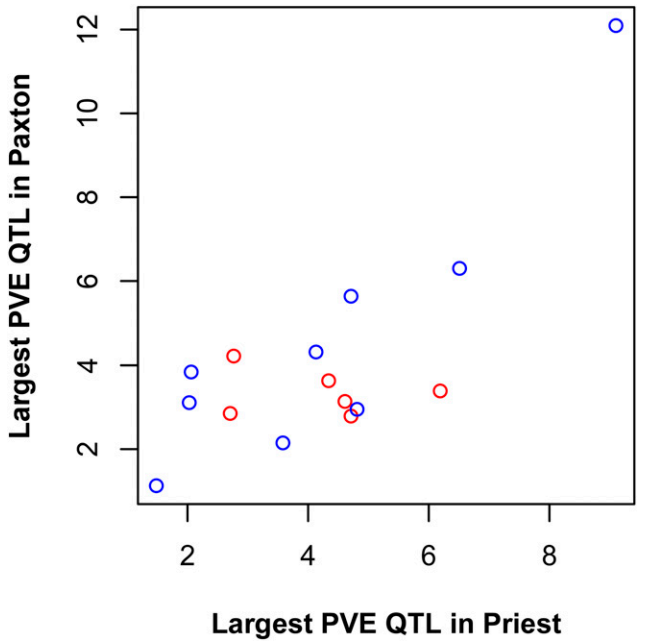

Figure 3 QTL effect size and genetic parallelism. The horizontal axis shows the percent of the phenotypic variance explained (PVE) by the largest effect QTL in Priest Lake underlying each trait having at least one QTL in both lakes ($N = 15$ traits). The same for Paxton Lake is shown on the vertical axis. Blue dots represent cases where the QTL is the same (maps to the same genomic location) in both lakes. Red dots represent cases where the QTL is different (maps to different genomic locations) in the two lakes.

What explains the prevalence of QTL reuse found to underlie parallel phenotypic evolution between the stickleback species pairs? First, the pairs are recently derived from a common ancestral population (~10,000–12,000 years ago) (Schluter and McPhail 1992; McPhail 1994; Taylor and McPhail 2000; Jones *et al.* 2012a). Genetic constraints (*e.g.*, the number and identity of loci capable of producing a particular phenotype), and genetic biases (*e.g.*, beneficial mutation rates, negative pleiotropic consequences, etc.) are likely to be very similar between them, increasing the probability that the same genes will underlie adaptive evolution (Conte *et al.* 2012). Second, in the case of threespine stickleback, prevalent QTL reuse may be due at least in part to the use of a shared pool of standing genetic variation. Previous

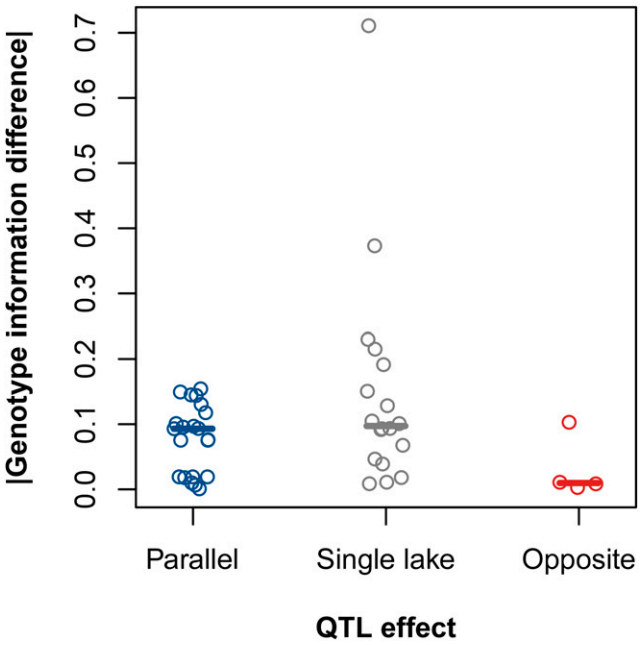

Figure 4 Difference in proportion of missing genotype information between crosses by QTL effect category. The absolute value of the difference in genotype information between the Paxton Lake cross and the Priest Lake cross at candidate QTL that were determined to have parallel effects (N = 21; blue), an effect in only a single lake (N = 18; gray), and opposite effects (N = 4; red). Solid lines represent medians for each group.

evidence suggests that the repeated evolution of many traits in freshwater threespine stickleback populations after colonization by the same marine ancestral form involved natural selection on shared standing genetic variation (Colosimo *et al.* 2005; Miller *et al.* 2007; Kitano *et al.* 2010; Jones *et al.* 2012b). On the other hand, definitive evidence for *de novo* mutations at the same locus underlying the independent evolution of similar phenotypes has also been observed in freshwater sticklebacks (Chan *et al.* 2010). However, we do not yet know the extent to which selection on standing variation *vs. de novo* mutation contributes to phenotypic evolution in the benthic–limnetic species pairs, in other stickleback populations, or in other species. The population genomic analyses of Jones *et al.* (2012b) found that ~35% of divergent genomic regions between a single marine-freshwater stickleback pair occurred at the same loci in multiple marine-freshwater population pairs. In the future, it will be crucial to investigate the relative importance of shared standing variation *vs. de novo* mutations to repeated phenotypic evolution in three-spine sticklebacks, as well as across independent natural populations in many systems.

Our quantitative, simultaneous-mapping approach using many morphological traits and including many small-effect QTL estimated surprisingly similar levels of gene reuse to those reported in the metaanalysis by Conte *et al.* (2012). Average proportional similarity of QTL use underlying parallel traits was 0.38 ± 0.07 SE in the current study, which is only slightly lower than the estimate of 0.47 ± 0.15 SE obtained in Conte *et al.* 2012) calculated from parallel traits mapped in young independent populations belonging to the same species. The metaanalysis estimate is based on multiple study systems, but only one or a few traits per system, in contrast to the present study of a large number of traits in a single system. The similarity of these estimates of QTL reuse based on different approaches suggests that gene reuse may be a robust and pervasive feature of adaptation in natural populations.

Nevertheless, our estimates might also be affected by several biases. First, QTL are relatively large genomic regions containing many genes, and some instances of parallel phenotypic evolution associated with QTL reuse might actually be caused by mutations in different, linked genes. Shared local mutation and recombination rates (Renaut *et al.* 2014) in addition to clustering of loci involved in local adaptation (Yeaman 2013) may cause different genes within the same genomic regions to sometimes underlie parallel phenotypic evolution. Consistent with this potential bias, other studies have found the highest repeatability of genetic evolution between independently diverged populations when large genomic regions are compared, moderate repeatability when individual genes are compared, and low repeatability when individual nucleotides are compared (Tenaillon *et al.* 2012; Renaut *et al.* 2014). However, in those studies it is not known whether the phenotypic effects of genomic changes are parallel. Second, our QTL analysis is based on only one cross per lake and therefore one individual per species. If QTL are polymorphic within species in one or both lakes, we may by chance find a QTL in one lake and not the other due to sampling error. This should occur inversely in relation to degree of allele fixation within each pair and the difference in QTL allele frequency between sympatric species. Nevertheless, our results should give an accurate picture of the probability of QTL reuse when averaged over many QTL. Third, pleiotropic effects of a single genetic change might have caused us to overestimate the number of independent QTL used in our analyses. Indeed, when we conducted QTL mapping of principal components rather than traits, we detected fewer QTL, yet they occurred in largely the same locations in the genome. This suggests that pleiotropy might indeed be present. Nevertheless, several uncorrelated principal components mapped to overlapping genomic locations, suggesting that multiple genetic changes might be present on some chromosomes. Furthermore, despite the possible effects of pleiotropy, accounting for it in our analyses did not greatly change our estimates of QTL reuse. Fourth, we may have missed some QTL with parallel and opposite effects if there was too little genotype information at a locus in one of the crosses but not the other. We found that the single-lake category included a small number of QTL having a large difference between the crosses in the proportion of missing genotype information (entropy differences). It is therefore possible that some parallel QTL have been classified as single-lake QTL in our analysis because of missing genotype information in a given chromosomal region in one of the two crosses.

However, based on the range of values observed for QTL with parallel and opposite effects, entropy differences corresponding to single-lake QTL appeared large enough to potentially mislead us in a relatively small number of cases (Figure 4). Fifth, the traits we mapped were mostly continuously varying, quantitative traits, underlain by mostly small effect loci. The closer the effect of a QTL is to a given detection threshold (either slightly above or below it), the less likely it is to be detected twice, because of sampling error. For this reason, small-effect QTL may have a tendency to be miscategorized as having an effect in only a single lake and we may have underestimated proportional similarity of QTL use between lakes. However, if this were the case, we would have expected an enrichment of small effect QTL in the single-lake QTL effect category, which we did not see.

We predicted that the probability of QTL reuse would depend on its effect size, assuming that phenotypic effect size is indicative of fitness effect size. Under fairly broad assumptions, if a new beneficial mutation independently fixes in two identical populations experiencing the same selection pressures, the probability it is the same mutation depends on the number of beneficial mutations available (Orr 2005). The number of available beneficial mutations of large effect is generally small compared with the number of beneficial small-effect mutations (Orr 2006). It follows that when a mutation fixes in two populations, the probability it is the same mutation should be higher when the effect size is relatively large than when it is relatively small. Although Orr (2005, 2006) explicitly considered *de novo* mutation, the qualitative expectation should still hold when beneficial mutations fix from standing variation as long as large effect beneficial mutations are rarer than those of small effect (Albert *et al.* 2008). We found no evidence in support of this prediction (Figure 3). However, we observed a tantalizing trend: the two traits having the largest QTL effects in both lakes indeed mapped to the same QTL (Figure 3). Small sample size, a small range of QTL effect sizes, and a noisy relationship between phenotypic and fitness effect sizes might explain why we found no evidence for the predicted effect.

Looking ahead, it will be important to combine forward genetic approaches that link genotypes to phenotypes (*i.e.*, QTL and association mapping) with population genomics studies to identify the specific genetic changes underlying parallel phenotypic changes. Such an approach will also allow use of phylogenetics to determine how often shared standing genetic variation is the cause of genetic parallelism. To date, relatively few population genomic studies provide quantitative estimates of parallel genomic changes, and these find somewhat lower estimates than we have observed. For example, 20% of genes experiencing mutations are shared across independent lines of experimentally evolved *Escherichia coli* populations adapting to similar environmental conditions (Tenaillon *et al.* 2012), 17% of divergent SNPs are shared across independent population pairs of stick insects (Soria-Carrasco *et al.* 2014), and 35% of the divergent genomic regions found in a single freshwater–marine comparison of threespine sticklebacks are shared across multiple freshwater–marine pairs (Jones *et al.* 2012b). However, while our approach addresses how often and to what extent the same loci underlie parallel adaptive evolution of specific phenotypes, the population genomic studies measure how often the same loci have acquired mutations in association with adaptation to a shared type of environment regardless of the specific phenotypic effects of mutations. A combination of the two approaches will enable fine-scale resolution of the genetics underlying parallel phenotypic evolution.

As we obtain more and better estimates of the repeatability of the genetics of adaptation across many systems, we will be able to ask what factors influence repeatability. For example, future studies should aim to estimate the *actual* number of genes in which mutations may lead to a particular phenotype, and then begin to dissect the genetic biases that will cause the *effective* number to be lower (Streisfeld and Rausher 2011). As our understanding of these factors improves, so will our ability to predict the genetics of adaptation.

Acknowledgments

We thank N. Bedford and T. Ingram for their assistance in the collection of F_2 hybrid fish and C. Sather for performing the SNP genotyping. We are also grateful to R. Svanback and J. Gow for providing wild-caught benthic and limnetic specimens (or photographs of specimens) from their collections. We thank Leonie Moyle and two anonymous reviewers for comments that greatly improved the manuscript. This work was supported by the National Science and Engineering Research Council (NSERC) CREATE training program and a University of British Columbia Zoology Graduate Fellowship (to G.L.C.), as well as grants from the National Institutes of Health (F32 GM086125 to M.E.A., P50 HG002568 to D.M.K. and C.L.P., and R01 GM089733 to D.S. and C.L.P.) and NSERC (D.S.).

Literature Cited

Albert, A. Y. K., S. Sawaya, T. H. Vines, A. K. Knecht, C. T. Miller *et al.*, 2008 The genetics of adaptive shape shift in stickleback: pleiotropy and effect size. Evolution 62: 76–85.

Arnegard, M. E., M. D. McGee, B. Matthews, K. B. Marchinko, G. L. Conte *et al.*, 2014 Genetics of ecological divergence during speciation. Nature 511: 307–311.

Broman, K. W., and S. Sen, 2009 *A Guide to QTL Mapping with R/qtl*, Springer-Verlag, New York.

Broman, K. W., and H. Wu, 2013 *QTL: Tools for Analyzing QTL Experiments*. CRAN: Comprehensive R Archive Network. Available at: http://www.r-project.org.

Burnham, K. P., and D. R. Anderson, 2002 *Model Selection and Multimodel Inference: A Practical Information-Theoretic Approach*, Springer-Verlag, New York.

Chan, Y. F., M. E. Marks, F. C. Jones, G. Villarreal, M. D. Shapiro *et al.*, 2010 Adaptive evolution of pelvic reduction in sticklebacks by recurrent deletion of a Pitx1 enhancer. Science 327: 302–305.

Colosimo, P. F., K. E. Hosemann, S. Balabhadra, G. Villarreal, M. Dickson *et al.*, 2005 Widespread parallel evolution in sticklebacks by repeated fixation of ectodysplasin alleles. Science 307: 1928–1933.

Conte, G. L., M. E. Arnegard, C. L. Peichel, and D. Schluter, 2012 The probability of genetic parallelism and convergence in natural populations. Proc. R. Soc. B Biol. Sci. **279:** 5039–5047.

Dryden, I. L., 2013 *Shapes: Statistical Shape Analysis*. CRAN: Comprehensive R Archive Network. Available at: http://www.r-project.org.

Endler, J. A., 1986 *Natural Selection in the Wild*, Princeton University Press, Princeton, NJ.

Fox, J., S. Weisberg, D. Adler, D. Bates, G. Baud-Bovy *et al.*, 2013 *car: Companion to Applied Regression*. CRAN: Comprehensive R Archive Network. Available at: http://www.r-project.org.

Gow, J. L., S. M. Rogers, M. Jackson, and D. Schluter, 2008 Ecological predictions lead to the discovery of a benthic–limnetic sympatric species pair of threespine stickleback in Little Quarry Lake, British Columbia. Can. J. Zool. 86: 564–571.

Hadfield, J., 2013 *Masterbayes: ML and MCMC methods for pedigree reconstruction and analysis*. CRAN: Comprehensive R Archive Network. Available at: http://www.r-project.org.

Harvey, P. H., and M. D. Pagel, 1991 *The Comparative Method in Evolutionary Biology*, Oxford University Press, Oxford.

Ingram, T., R. Svanbäck, N. J. B. Kraft, P. Kratina, L. Southcott *et al.*, 2012 Intraguild predation drives evolutionary niche shift in threespine stickleback. Evolution 66: 1819–1832.

Jones, F. C., Y. F. Chan, J. Schmutz, J. Grimwood, S. D. Brady *et al.*, 2012a A genome-wide SNP genotyping array reveals patterns of global and repeated species-pair divergence in sticklebacks. Curr. Biol. 22: 83–90.

Jones, F. C., M. G. Grabherr, Y. F. Chan, P. Russell, E. Mauceli *et al.*, 2012b The genomic basis of adaptive evolution in threespine sticklebacks. Nature 484: 55–61.

Kitano, J., S. C. Lema, J. A. Luckenbach, S. Mori, Y. Kawagishi *et al.*, 2010 Adaptive divergence in the thyroid hormone signaling pathway in the stickleback radiation. Curr. Biol. 20: 2124–2130.

Losos, J. B., 2011 Convergence, adaptation, and constraint. Evolution 65: 1827–1840.

Lynch, M., and B. Walsh, 1998 *Genetics and Analysis of Quantitative Traits*, Sinauer Associates, Sunderland, MA.

Martin, A., and V. Orgogozo, 2013 The loci of repeated evolution: a catalog of genetic hotspots of phenotypic variation. Evolution 67: 1235–1250.

McKinnon, J. S., and H. D. Rundle, 2002 Speciation in nature: the threespine stickleback model systems. Trends Ecol. Evol. 17: 480–488.

McPhail, J. D., 1984 Ecology and evolution of sympatric sticklebacks (Gasterosteus): morphological and genetic evidence for a species pair in Enos Lake, British Columbia. Can. J. Zool. 62: 1402–1408.

McPhail, J. D., 1992 Ecology and evolution of sympatric sticklebacks (Gasterosteus): evidence for a species pair in Paxton Lake, Texada Island, British Columbia. Can. J. Zool. 70: 361–369.

McPhail, J. D., 1994 Speciation and the evolution of reproductive isolation in the sticklebacks (Gasterosteus) of south-western British Columbia, pp. 399–437 in *The Evolutionary Biology of the Threespine Stickleback*, edited by M. A. Bell, and S. A. Foster. Oxford University Press, Oxford.

Miller, C. T., S. Beleza, A. A. Pollen, D. Schluter, R. A. Kittles *et al.*, 2007 Cis-regulatory changes in kit ligand expression and parallel evolution of pigmentation in sticklebacks and humans. Cell 131: 1179–1189.

Ooijen, J. W., and R. E. Voorrips, 2002 *JoinMap: Version 3.0: Software for the Calculation of Genetic Linkage Maps*, Plant Research International, Wageningen, The Netherlands.

Orr, H. A., 2005 The probability of parallel evolution. Evolution 59: 216–220.

Orr, H. A., 2006 The distribution of fitness effects among beneficial mutations in Fisher's geometric model of adaptation. J. Theor. Biol. 238: 279–285.

Peichel, C. L., K. S. Nereng, K. A. Ohgi, B. L. E. Cole, P. F. Colosimo *et al.*, 2001 The genetic architecture of divergence between threespine stickleback species. Nature 414: 901–905.

Renaut, S., G. L. Owens, and L. H. Rieseberg, 2014 Shared selective pressure and local genomic landscape lead to repeatable patterns of genomic divergence in sunflowers. Mol. Ecol. 23: 311–324.

Rohlf, F. J., 2010 *tpsDig*. Department of Ecology and Evolution, State University of New York at Stony Brook, Stony Brook, NY.

Schluter, D., 2000 *The Ecology of Adaptive Radiation*, Oxford University Press, Oxford.

Schluter, D., and J. D. McPhail, 1992 Ecological character displacement and speciation in sticklebacks. Am. Nat. 140: 85–108.

Schluter, D., and L. M. Nagel, 1995 Parallel speciation by natural selection. Am. Nat. 146: 292–301.

Soria-Carrasco, V., Z. Gompert, A. A. Comeault, T. E. Farkas, T. L. Parchman *et al.*, 2014 Stick insect genomes reveal natural selection's role in parallel speciation. Science 344: 738–742.

Stern, D. L., 2013 The genetic causes of convergent evolution. Nat. Rev. Genet. 14: 751–764.

Stern, D. L., and V. Orgogozo, 2008 The loci of evolution: How predictable is genetic evolution? Evolution 62: 2155–2177.

Streisfeld, M. A., and M. D. Rausher, 2011 Population genetics, pleiotropy, and the preferential fixation of mutations during adaptive evolution. Evolution 65: 629–642.

Taylor, E. B., and J. D. McPhail, 2000 Historical contingency and ecological determinism interact to prime speciation in sticklebacks, Gasterosteus. Proc. R. Soc. Lond. B Biol. Sci. 267: 2375–2384.

Tenaillon, O., A. Rodríguez-Verdugo, R. L. Gaut, P. McDonald, A. F. Bennett *et al.*, 2012 The molecular diversity of adaptive convergence. Science 335: 457–461.

Yeaman, S., 2013 Genomic rearrangements and the evolution of clusters of locally adaptive loci. Proc. Natl. Acad. Sci. USA 110: E1743–E1751.

Communicating editor: L. Moyle

GENETICS

Supporting Information
www.genetics.org/lookup/suppl/doi:10.1534/genetics.115.182550/-/DC1

Extent of QTL Reuse During Repeated Phenotypic Divergence of Sympatric Threespine Stickleback

Gina L. Conte, Matthew E. Arnegard, Jacob Best, Yingguang Frank Chan, Felicity C. Jones, David M. Kingsley, Dolph Schluter, and Catherine L. Peichel

DOI: 10.1534/genetics.115.182550

Supplementary Material

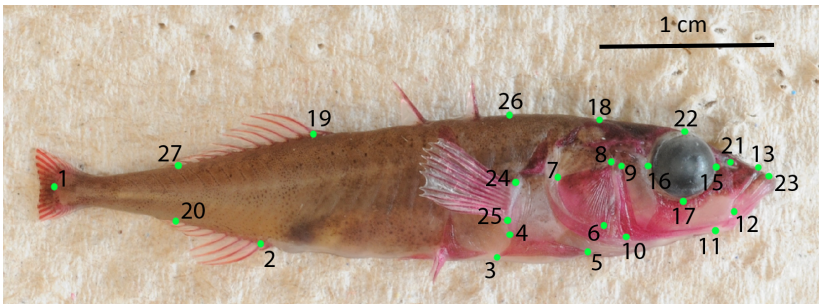

Landmarks (x and y coordinates)

1. posterior midpoint of the caudal peduncle
2. anterior insertion of the anal fin at the first soft ray
3. posteroventral corner of the ectocoracoid bone
4. posterodorsal corner of the ectocoracoid bone
5. anterior-most corner of the ectocoracoid bone
6. anteroventral corner of the opercle
7. posterodorsal corner of the opercle
8. dorsal edge of the opercle-hyomandibular boundary
9. dorsal-most extent of the preopercle
10. posteroventral corner of the preopercle
11. anterior-most extent of the preopercle along the ventral silhouette
12. posteroventral extent of the maxilla
13. anterodorsal extent of the maxilla
14. *No landmark*
15. anterior margin of the orbit in line with the eye's midpoint
16. posterior margin of the orbit in line with the eye's midpoint
17. ventral margin of the orbit in line with the eye's midpoint
18. posterior extent of neurocranium (i.e., supraoccipital) along dorsal silhouette
19. anterior insertion of the dorsal fin at the first soft ray
20. posterior insertion of the anal fin at the first soft ray
21. edge of the lachrymal at the naris
22. dorsal margin of the orbit in line with the eye's midpoint
23. anterior-most extent of the premaxilla
24. dorsal insertion of the pectoral fin
25. ventral insertion of the pectoral fin
26. dorsum of the trunk over the pectoral fin midpoint
27. posterior insertion of the dorsal fin at the first soft ray

- centroid size (square root of the sum of squared distances of the 26 landmarks from their centroid)

Meristics

- lateral plate count
- 1st dorsal spine presence/absence
- 2nd dorsal spine presence/absence
- long gill raker count (on the first gill arch)
- short gill raker count (on the first gill arch)

Figure S1 All phenotypes scored

Landmark numbers were made consistent with those in Arnegard et al. (2014).

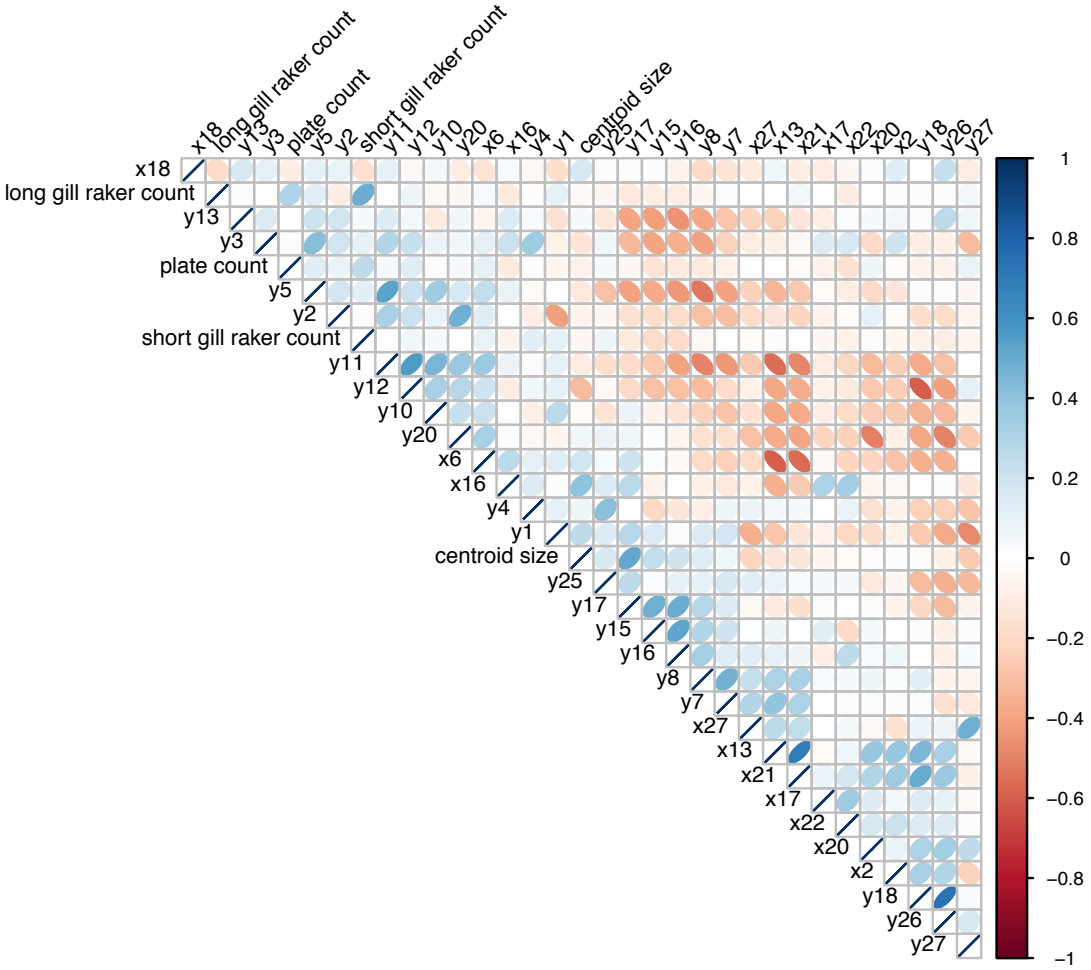

Figure S2 Correlations among parallel traits in Paxton Lake F_2s

The strength of correlation between pairs of parallel traits in Paxton Lake F_2s is indicated by both color and elongation of the ellipse. F_2 values were corrected for family and sex.

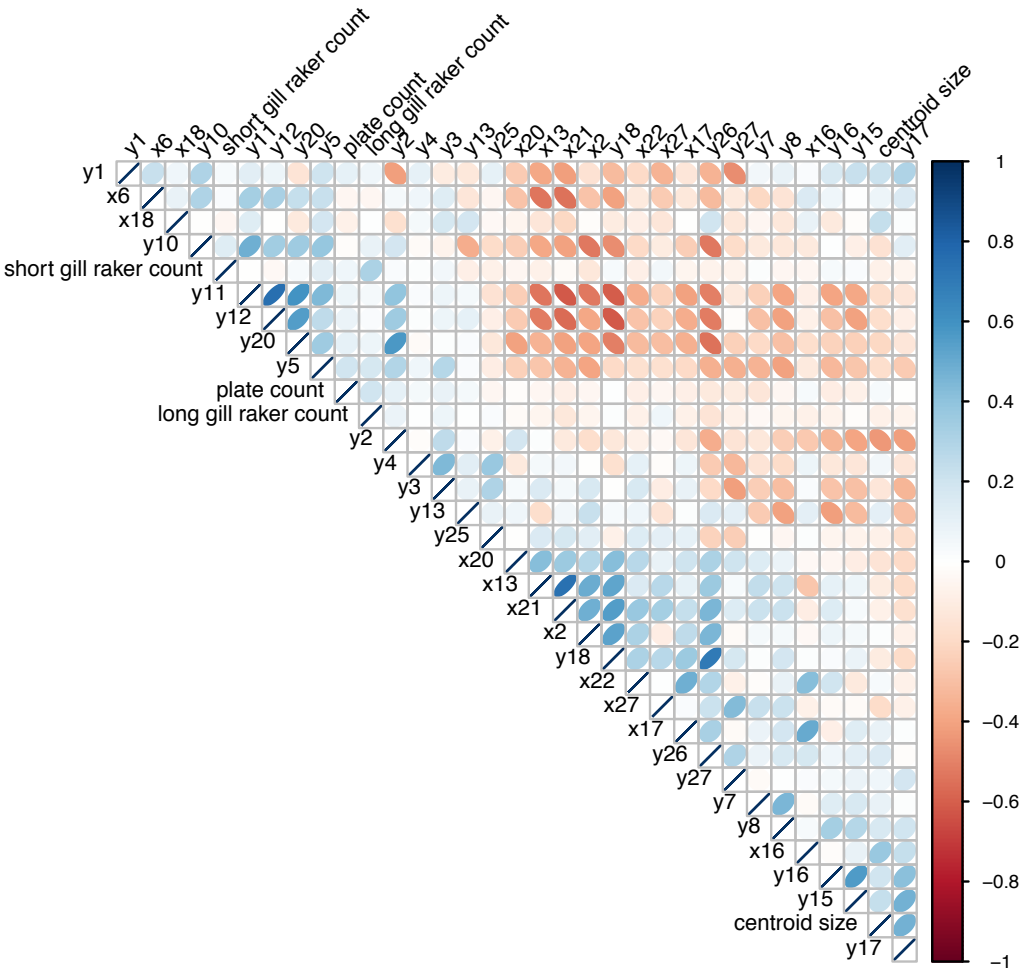

Figure S3 Correlations among parallel traits in Priest Lake F_2s

The strength of correlation between pairs of parallel traits in Priest Lake F_2s is indicated by both color and elongation of the ellipse. F_2 values were corrected for family and sex.

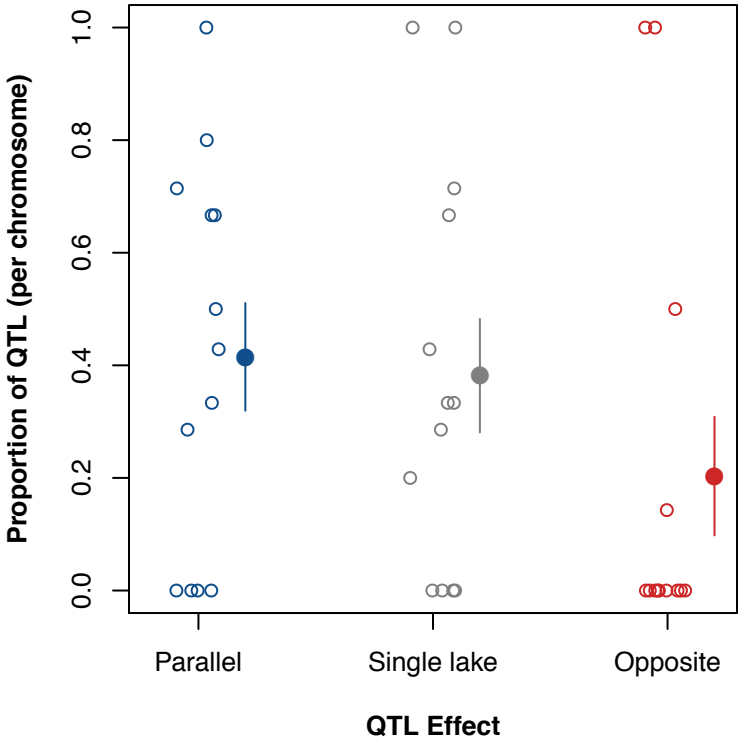

Figure S4 Proportions of QTL effect categories per chromosome

The proportion of parallel (blue), single lake (gray) and opposite QTL effects (red) on 13 chromosomes (Figure 2). Filled circles and vertical lines indicate the mean proportion and SE over the 13 chromosomes: 41.5% ± 9.6% SE parallel, 38.1% ± 10.1% SE single lake, and 20.3% ± 10.5% SE opposite effects.

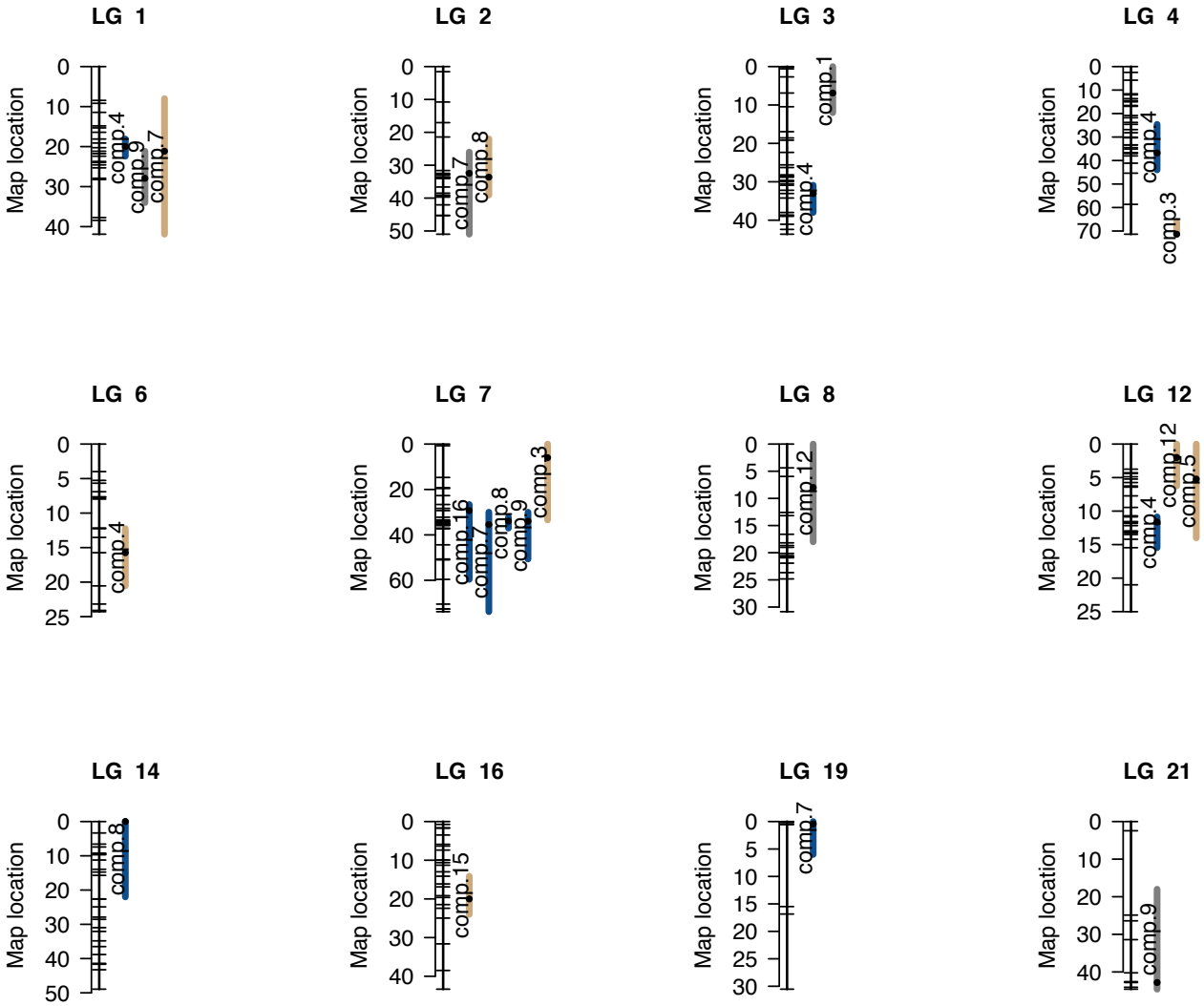

Figure S5 Map of Principal Component QTL

Map of 23 QTL (i.e. QTL with an effect in one or both lakes) underlying parallel principal components of parallel traits. Only QTL for principal components accounting for the first 90% of cumulative variance in F_2 phenotypes are shown. Linkage groups on which QTL were detected are shown. For each, the positions of SNPs markers in the combined Paxton and Priest linkage map are depicted by tick marks on the left. Colored bars span the 1.5 LOD confidence intervals of QTL. Black dots within bars represent the peak marker position. The principal component phenotype affected by each QTL is indicated to the left its bar. Colors of bars represent the 'QTL Effect' category, as follows: parallel effects – blue; effect in only one lake – grey; opposite effects – red. Tan colored bars represent the candidate QTL for which more than one QTL effect category fit the data nearly equally well.

Table S1 Trait divergence categories

(Starts on next page) Trait divergence was considered 'parallel' when the best model of the species effect was either 'same effect' or was 'different effect' and the direction of divergence was 'same'. Trait divergence was considered 'single lake' when the best model of the species effect was either 'effect only in Paxton' or 'effect only in Priest'. Trait divergence was considered 'opposite' when the best model of species effect was 'different effect' and the direction of divergence was 'opposite'. The second best model of species effect and the delta AICc between it and the best model is also shown. When the delta AICc was less than two and the 2nd best model called for a different trait divergence category than the best model, we dropped the trait from further study (indicated by 'NA' in the ''Trait divergence' based on AICc model selection' column), though detected QTL for all traits measured are shown in Tables S2 – S4.

Trait	'Trait divergence' based on AICc model selection	Direction of divergence	Best model of species effect	2nd best model of species effect	Delta AICc
plate count	Parallel	same	different effect	same effect	35.62
gill raker count	Parallel	same	same effect	different effect	1.24
1st dorsal spine	Single lake	opposite	effect in Paxton only	different effect	2.14
2nd dorsal spine	NA	same	no effect	effect in Priest only	0.95
x1	NA	opposite	no effect	effect in Priest only	0.17
y1	Parallel	same	same effect	different effect	1.72
x2	Parallel	same	different effect	same effect	5.78
y2	Parallel	same	same effect	different effect	1.28
x3	Opposite	opposite	different effect	effect in Paxton only	3.97
y3	Parallel	same	different effect	same effect	1.14
x4	Single lake	opposite	effect in Priest only	different effect	2.12
y4	Parallel	same	different effect	same effect	31.59
x5	NA	opposite	effect in Priest only	different effect	0.02
y5	Parallel	same	different effect	same effect	2.77
x6	Parallel	same	same effect	different effect	2.20
y6	Opposite	opposite	different effect	effect in Priest only	5.36
x7	NA	opposite	different effect	effect in Priest only	1.47
y7	Parallel	same	same effect	different effect	1.90
x8	NA	opposite	effect in Paxton only	different effect	0.32
y8	Parallel	same	different effect	same effect	0.53
x9	NA	same	effect in Priest only	different effect	1.36
y9	NA	same	effect in Paxton only	different effect	0.26
x10	Single lake	same	effect in Priest only	different effect	2.18
y10	Parallel	same	same effect	different effect	1.01
x11	NA	same	effect in Paxton only	different effect	1.69
y11	Parallel	same	same effect	different effect	1.83
x12	Opposite	opposite	different effect	effect in Priest only	19.50
y12	Parallel	same	same effect	different effect	1.03
x13	Parallel	same	different effect	same effect	2.97
y13	Parallel	same	same effect	different effect	1.72
x15	NA	same	same effect	effect in Priest only	1.70
y15	Parallel	same	same effect	different effect	1.01
x16	Parallel	same	different effect	same effect	0.78
y16	Parallel	same	same effect	different effect	0.67
x17	Parallel	same	different effect	same effect	3.19
y17	Parallel	same	different effect	same effect	0.37
x18	Parallel	same	different effect	same effect	0.84
y18	Parallel	same	different effect	same effect	0.43
x19	NA	opposite	different effect	effect in Priest only	1.00
y19	Single lake	same	effect in Paxton only	different effect	2.13
x20	Parallel	same	different effect	effect in Priest only	3.10
y20	Parallel	same	different effect	same effect	17.17

Trait	'Trait divergence' based on AICc model selection	Direction of divergence	Best model of species effect	2nd best model of species effect	Delta AICc
x21	Parallel	same	same effect	different effect	2.09
y21	NA	opposite	no effect	effect in Priest only	0.37
x22	Parallel	same	same effect	different effect	2.17
y22	NA	same	effect in Paxton only	different effect	0.27
x23	Opposite	opposite	different effect	effect in Paxton only	4.95
y23	NA	same	different effect	effect in Priest only	0.29
x24	NA	same	effect in Priest only	different effect	1.32
y24	Opposite	opposite	different effect	effect in Paxton only	17.01
x25	Single lake	same	effect in Priest only	different effect	2.19
y25	Parallel	same	different effect	effect in Paxton only	4.15
x26	NA	same	different effect	effect in Priest only	1.63
y26	Parallel	same	different effect	same effect	3.30
x27	Parallel	same	same effect	different effect	2.12
y27	Parallel	same	same effect	different effect	2.15
centroid	Parallel	same	different effect	effect in Paxton only	25.59

Table S2 Identities, map positions, and physical locations of SNPs

(Starts on next page) Identities, map positions, and physical locations of the 430 single nucleotide polymorphism (SNP) markers used in linkage and QTL analysis. The linkage group (LG) and map position in centimorgans (cM) are provided for each SNP. Each marker name is a combination of the chromosome number (before the colon) and the physical position in base pairs (after the colon) of the SNP in the reference stickleback genome assembly (Broad S1, Feb. 2006) (Jones et al. 2012). Markers identified from unassembled regions of the genome are indicated with 'chrUN'. In such cases, the position in base pairs is based on the composite chrUN in the UCSC genome browser. Marker information can be obtained from the Single Nucleotide Polymorphism Database (dbSNP, available at http://www.ncbi.nlm.nih.gov/projects/SNP/), which is hosted by the National Center for Biotechnology Information (NCBI) of the U.S. National Institutes of Health. Data for specific markers may be found by searches of the dbSNP using the submitted SNP ID numbers (ss#). Two SNPs are still awaiting ss# assignment.

Linkage Group	Map Position (cM)	Marker name (chromosome: position)	NCBI submitted SNP ID numbers (ss#)	Linkage Group	Map Position (cM)	Marker name (chromosome: position)	NCBI submitted SNP ID numbers (ss#)
1	0	chrI:27642534	418642015	2	45.24	chrII:919438	244222781
1	8.45	chrUn:18660323	418642624	2	45.324	chrUn:23384875	418642627
1	9.18	chrI:22716347	418642010	2	50.981	chrII:533883	120258418
1	11.439	chrI:3310077	244222768	3	0	chrUn:30223426	418642641
1	14.833	chrI:19946499	418642005	3	0.219	chrUn:27149198	418642632
1	15.322	chrI:2718044	418641984	3	0.593	chrUn:27040022	418642631
1	16.421	chrI:4219350	244222770	3	2.685	chrUn:30323959	418642642
1	18.111	chrI:3494580	120258412	3	6.884	chrIII:16463929	244222796
1	19.109	chrI:14261764	418641998	3	10.455	chrIII:16251071	120258431
1	20.267	chrI:15145305	418642000	3	16.956	chrIII:15793968	418642089
1	21.162	chrI:4171190	244222769	3	18.59	chrIII:15185662	418642088
1	21.745	chrI:17306554	418642003	3	19.173	chrIII:15157782	418642087
1	22.395	chrI:7545826	418641993	3	22.347	chrIII:14892994	244222794
1	23.715	chrI:20584613	418642006	3	25.596	chrIII:13397314	418642078
1	23.959	chrI:22899825	418642011	3	26.289	chrIII:13520975	252841102
1	24.572	chrI:22361077	120258417	3	28.19	chrIII:14393183	418642084
1	25.305	chrI:3538018	418641987	3	28.59	chrIII:14048561	252841058
1	27.917	chrI:26879230	244222777	3	28.741	chrIII:13911180	418642080
1	28.238	chrI:25560380	418642013	3	28.761	chrIII:11836494	418642072
1	37.745	chrI:1550	418641979	3	29.684	chrIII:13699701	418642079
1	38.432	chrUn:37631434	244223001	3	29.727	chrIII:12930427	418642076
1	41.893	chrI:913033	120258411	3	29.906	chrIII:14135608	418642081
2	0	chrII:22443700	244222787	3	30.523	chrIII:14456990	252841063
2	1.55	chrII:22644752	418642054	3	30.9	chrIII:14248039	418642083
2	10.77	chrII:21231538	244222786	3	32.208	chrIII:11302839	418642071
2	17.049	chrII:21013052	418642052	3	33.049	chrIII:2376699	418642065
2	21.421	chrII:19985741	244222785	3	34.228	chrIII:1968625	418642063
2	31.618	chrII:5914538	418642030	3	37.992	chrIII:1198125	120258428
2	32.478	chrII:10092618	418642034	3	38.662	chrIII:639237	418642059
2	32.693	chrII:8305286	418642033	3	38.988	chrIII:1651721	252841079
2	33.053	chrII:6475468	244222782	3	41.069	chrIII:269753	418642057
2	33.629	chrII:17453243	418642042	3	42.403	chrIII:105665	418642055
2	33.653	chrII:5935944	252841148	3	43.645	chrIII:186390	418642056
2	33.707	chrII:12292176	120258425	4	0	chrUn:27478064	244222993
2	33.978	chrII:14611516	244222784	4	2.47	chrUn:27589750	418642633
2	34.026	chrII:17312835	418642041	4	5.799	chrUn:27402745	252841068
2	36.632	chrII:4530808	120258423	4	11.6	chrIV:32592491	418642150
2	38.498	chrII:19324477	418642044	4	12.021	chrIV:32487875	244222812
2	39.102	chrII:3931852	418642025	4	13.638	chrIV:32387818	120258447
2	39.262	chrII:4157699	252841112	4	14.49	chrIV:32277841	418642146
2	39.701	chrII:3516452	120258422	4	15.02	chrIV:32236655	418642145
2	42.057	chrII:3384330	120258421	4	16.56	chrIV:32092919	252841132

Linkage Group	Map Position (cM)	Marker name (chromosome: position)	NCBI submitted SNP ID numbers (ss#)	Linkage Group	Map Position (cM)	Marker name (chromosome: position)	NCBI submitted SNP ID numbers (ss#)
4	16.927	chrIV:32005807	120258445	5	46.025	chrV:7791830	252841093
4	20.838	chrIV:31740478	244222809	5	50.516	chrUn:10540032	418642614
4	21.77	chrIV:31350187	418642140	5	53.473	chrUn:10213240	418642613
4	23.776	chrIV:29763654	120258443	5	53.596	chrUn:11980918	252841136
4	24.599	chrIV:31611147	252841084	5	56.444	chrUn:12390868	120258569
4	26.831	chrIV:30568387	252841083	6	0	chrVI:487411	418642183
4	28.149	chrIV:5165268	418642111	6	3.991	chrVI:6312798	418642187
4	30.064	chrIV:21232476	418642127	6	5.262	chrVI:1440771	244222823
4	30.311	chrIV:21605258	252841082	6	5.672	chrVI:10415741	418641920
4	33.352	chrIV:15721538	244222806	6	6.903	chrVI:11954719	418642192
4	33.352	chrIV:15737291	244222807	6	7.644	chrVI:13220597	252841044
4	34.536	chrIV:15530121	244222805	6	7.721	chrVI:11873663	120258454
4	35.12	chrIV:15052901	244222804	6	7.97	chrVI:12427477	418642193
4	36.67	chrIV:10997988	244222801	6	12.157	chrVI:3116218	244222825
4	36.782	chrIV:9220132	418642120	6	12.259	chrVI:16870159	244222834
4	36.984	chrIV:8545605	418642119	6	13.529	chrVI:218630	244222820
4	38.029	chrIV:11367975	120258435	6	15.74	chrVI:14571427	418642200
4	41.136	chrIV:4065598	244222799	6	20.547	chrVI:15413799	418642203
4	45.377	chrIV:3334208	418642103	6	23.176	chrVI:14976508	418642201
4	58.662	chrIV:2045971	418642099	6	24.097	chrVI:15654034	418642204
4	71.359	chrIV:219384	418642093	6	24.282	chrVI:15692312	418642205
5	0	chrUn:25831365	418642629	7	0	chrVII:27918897	418642257
5	2.542	chrUn:25946639	244222990	7	0.743	chrUn:29400087	418642638
5	8.438	chrV:11316476	252841077	7	14.707	chrVII:26769148	418642251
5	9.302	chrV:11368893	418642177	7	19.214	chrVII:26538823	244222842
5	13.732	chrV:11509827	418642178	7	19.55	chrVII:26448674	252841125
5	17.208	chrV:11642284	418642179	7	22.7	chrVII:26227403	120258461
5	19.847	chrV:11722274	418642180	7	26.614	chrVII:25662266	120258460
5	20.126	chrV:10649179	252841089	7	28.341	chrVII:25193081	418642246
5	23.802	chrV:10674055	418642173	7	29.302	chrVII:24988330	
5	30.785	chrV:10028353	418642167	7	32.219	chrVII:24217606	418642245
5	31.771	chrV:9884672	418642164	7	33.407	chrVII:19857837	418642237
5	31.771	chrV:9911653	418642165	7	33.931	chrVII:16848769	418642232
5	32.969	chrV:9768052	252841108	7	34.008	chrVII:24203557	120258459
5	34.423	chrV:9157076	244222818	7	34.209	chrVII:23703797	418642243
5	40.776	chrV:8327818	244222816	7	34.447	chrVII:22798737	418642240
5	42.038	chrV:1238066	120258448	7	34.985	chrVII:21302029	418642238
5	43.017	chrV:1727383	418642153	7	35.124	chrVII:20883742	252841067
5	43.695	chrV:2528528	244222814	7	35.45	chrVII:18353106	244222839
5	44.689	chrUn:11085407	418642615	7	35.809	chrVII:13452516	244222836
5	45.499	chrV:5064057	418642160	7	35.815	chrVII:5552972	252841066
5	45.501	chrV:4819972	418642158	7	37.029	chrVII:5936068	120258457

Linkage Group	Map Position (cM)	Marker name (chromosome: position)	NCBI submitted SNP ID numbers (ss#)	Linkage Group	Map Position (cM)	Marker name (chromosome: position)	NCBI submitted SNP ID numbers (ss#)
7	37.322	chrVII:4310181	418642225	9	32.728	chrIX:13852312	418642311
7	44.369	chrVII:2559099	418642220	9	33.542	chrIX:803523	252841065
7	50.636	chrVII:1569236	418642218	9	33.594	chrIX:16779825	244222869
7	50.989	chrVII:1481322	418642217	9	36.679	chrIX:2360337	244222859
7	59.593	chrVII:835236	252841091	9	37.317	chrIX:2310926	418642299
7	70.492	chrUn:29087782	244222996	9	39.339	chrIX:2089567	244222858
7	72.645	chrVII:537136	252841113	9	43.455	chrIX:1273244	244222857
7	72.679	chrVII:393417	418642213	9	45.903	chrIX:1417909	418642292
7	73.819	chrUn:28671327	244222995	9	46.308	chrIX:1571056	418642294
8	0	chrVIII:19282658	418642286	9	52.345	chrIX:639609	244222856
8	4.379	chrVIII:868226	418642258	10	0	chrX:1275840	418642326
8	5.961	chrVIII:18760705	244222855	10	4.412	chrX:14831394	418642358
8	12.586	chrVIII:2505620	418642263	10	4.526	chrX:14456479	252841100
8	13.173	chrVIII:1929053	244222843	10	4.527	chrX:14549101	252841122
8	16.606	chrVIII:2257915	418642261	10	6.198	chrX:14265366	120258486
8	18.186	chrVIII:3765115	418642265	10	7.06	chrUn:14127611	418642619
8	18.689	chrVIII:3627706	244222844	10	8.977	chrUn:14043112	418642618
8	19.011	chrVIII:3987295	120258464	10	9.768	chrUn:24511995	418642628
8	20.132	chrVIII:6680213	418642268	10	10.14	chrUn:29017220	418642637
8	20.538	chrVIII:8858242	418642273	10	10.338	chrX:13132917	418642352
8	20.747	chrVIII:14278829	418642277	10	16.368	chrX:10080391	418642338
8	20.771	chrVIII:12472630	252841158	10	16.858	chrX:11139448	252841128
8	20.929	chrVIII:13412707	244222846	10	17.302	chrX:4696470	418642330
8	21.923	chrVIII:15261158	418642279	10	19.902	chrX:8703061	120258485
8	23.667	chrVIII:13577518	252841097	10	20.486	chrX:7113953	120258483
8	24.825	chrVIII:14472465	244222848	10	22.444	chrX:11252137	244222875
8	30.855	chrVIII:16843576	418642285	10	24.019	chrX:12844036	418642350
9	0	chrIX:19781202	244222870	10	28.446	chrX:12507632	244222877
9	0.675	chrIX:20090929	244222871	11	0	chrXI:16701186	244222888
9	7.45	chrIX:19745222	418642321	11	0.287	chrXI:16655205	120258495
9	17.662	chrIX:18494397	418642317	11	8.458	chrXI:15154801	418642382
9	19.295	chrIX:18826248	418642319	11	15.6	chrUn:32523521	418642646
9	19.628	chrIX:19322448	418642320	11	20.238	chrXI:14631875	418642379
9	24.547	chrIX:5109672	244222860	11	20.482	chrXI:14691162	418642380
9	25.033	chrIX:4882924	120258472	11	20.626	chrXI:14830913	244222885
9	27.249	chrIX:5403530	120258474	11	23.738	chrXI:15005173	244222886
9	28.314	chrIX:5568375	244222863	11	31.588	chrXI:12097498	418642375
9	30.384	chrIX:12933483	244222865	11	31.877	chrXI:10976029	244222883
9	30.606	chrIX:7146708	418642304	11	34.655	chrXI:9039275	252841094
9	31.139	chrIX:15670033	244222868	11	35.303	chrXI:7355052	418642370
9	31.408	chrIX:7893416	418642306	11	37.738	chrXI:12746496	244222884
9	31.862	chrIX:13553866	252841127	11	38.425	chrXI:3120961	244222880

Linkage Group	Map Position (cM)	Marker name (chromosome: position)	NCBI submitted SNP ID numbers (ss#)	Linkage Group	Map Position (cM)	Marker name (chromosome: position)	NCBI submitted SNP ID numbers (ss#)
11	42.418	chrXI:1017481	120258488	13	21.03	chrXIII:2632698	244222901
11	43.126	chrXI:1449684	120258489	13	22.175	chrXIII:2523163	120258505
11	43.715	chrXI:1266618	418642362	13	23.993	chrXIII:1909687	244222900
11	46.473	chrXI:234849	120258487	13	24.529	chrXIII:1698554	418642421
12	0	chrXII:17758877	244222897	13	27.703	chrXIII:1001571	120258503
12	3.744	chrXII:16628544	418642412	13	28.789	chrXIII:2105469	418642423
12	4.281	chrXII:2242677	418642394	14	0	chrXIV:14049917	252841090
12	4.39	chrUn:26305459	244222991	14	3.337	chrUn:21213332	120258571
12	4.88	chrXII:16877465	418642413	14	6.577	chrXIV:11054767	120258517
12	5.223	chrXII:3026329	418642398	14	7.427	chrXIV:9742642	418642458
12	5.738	chrXII:18221941	244222899	14	9.222	chrXIV:6992838	418642456
12	6.258	chrXII:4123972	418642400	14	9.409	chrXIV:15137805	418642462
12	6.422	chrUn:30606854	244222997	14	9.506	chrXIV:6641188	418642455
12	7.731	chrUn:38378170	120258576	14	9.686	chrXIV:7313827	418642457
12	9.452	chrXII:3810254	418642399	14	11.233	chrXIV:15033103	418642461
12	10.731	chrXII:6012527	418642404	14	13.935	chrXIV:3414352	120258514
12	10.731	chrXII:5828898	418642403	14	14.748	chrXIV:3598443	418642452
12	10.863	chrXII:5521301	418642402	14	15.715	chrXIV:3534175	120258515
12	11.573	chrXII:6399147	252841133	14	22.579	chrXIV:2084777	418642446
12	11.61	chrXII:6924609	418642405	14	22.648	chrXIV:1798136	418642443
12	11.639	chrXII:6745006	244222892	14	24.911	chrXIV:1713227	120258513
12	11.825	chrXII:6913126	120258500	14	27.904	chrXIV:1641269	418642442
12	12.164	chrXII:7504339	418642406	14	28.549	chrXIV:1442872	120258512
12	13.016	chrXII:16454328	418642411	14	30.976	chrXIV:1383447	244222908
12	13.016	chrXII:1589655	120258497	14	32.066	chrXIV:1311694	418642441
12	13.016	chrXII:2157795	418642393	14	34.828	chrXIV:1087388	418642439
12	13.016	chrXII:15046849	418642410	14	36.498	chrXIV:800076	418642438
12	13.24	chrXII:11472159	418642407	14	38.817	chrXIV:721170	244222907
12	13.498	chrXII:13045611	244222894	14	41.408	chrXIV:451065	120258511
12	14.199	chrXII:14223760	244222895	14	41.654	chrXIV:348659	418642435
12	15.462	chrXII:1483544	244222889	14	43.257	chrUn:35285565	418642649
12	20.999	chrXII:880748	418642389	14	48.931	chrUn:36334731	244223000
12	25.007	chrXII:548804	252841119	15	0	chrXV:13047331	418642481
13	0	chrXIII:18470329	252841124	15	0.602	chrXV:12281774	418642480
13	8.132	chrXIII:17392141	120258510	15	3.131	chrXV:6446874	418642477
13	8.48	chrXIII:17249562	418642432	15	6.668	chrXV:2507809	244222914
13	16.245	chrXIII:8085851	418642430	15	7.328	chrXV:3703641	418642475
13	17.207	chrXIII:4401535	418642425	15	9.649	chrXV:2169610	244222912
13	18.717	chrXIII:4868788	418642428	15	12.33	chrXV:1902350	244222911
13	19.246	chrXIII:4621027	418642426	15	13.521	chrXV:1800560	418642468
13	20.037	chrXIII:2969182	418642424	15	19.973	chrXV:414608	120258519
13	20.712	chrXIII:3109522	120258506	15	20.789	chrXV:505537	418642465

Linkage Group	Map Position (cM)	Marker name (chromosome: position)	NCBI submitted SNP ID numbers (ss#)	Linkage Group	Map Position (cM)	Marker name (chromosome: position)	NCBI submitted SNP ID numbers (ss#)
15	26.144	chrXV:979445	418642466	17	27.817	chrXVII:12022612	120258536
15	28.551	chrXV:215800	418642464	17	29.614	chrXVII:1264852	418642508
15	29.834	chrXV:11818	418642463	17	30.48	chrXVII:12528572	252841151
16	0	chrXVI:2764206	120258523	17	34.32	chrXVII:769372	244222939
16	0.74	chrXVI:2650854	244222922	17	34.515	chrXVII:645029	418642506
16	1.67	chrXVI:2392758	244222921	17	41.148	chrXVII:14127979	418642528
16	1.674	chrXVI:2483136	252841051	18	0	chrXVIII:15478444	120258549
16	3.48	chrXVI:3206769	244222923	18	19.259	chrXVIII:13773116	418642545
16	5.889	chrXVI:13588796	244222930	18	23.155	chrXVIII:13753579	244222958
16	6.329	chrXVI:14093156	244222931	18	24.456	chrXVIII:13193140	244222957
16	7.378	chrXVI:14963879	244222933	18	24.798	chrXVIII:12818939	120258545
16	9.956	chrXVI:12996432	244222929	18	26.138	chrXVIII:12273872	252841150
16	9.978	chrXVI:5562355	244222924	18	26.312	chrXVIII:11896010	244222954
16	10.609	chrXVI:6415385	418642487	18	27.539	chrXVIII:11765327	120258543
16	11.281	chrXVI:9428786	244222926	18	27.765	chrXVIII:11702469	418642543
16	12.994	chrXVI:13148331	418642492	18	27.765	chrXVIII:11641450	244222953
16	14.134	chrXVI:14283264	244222932	18	28.292	chrXVIII:11504306	418642542
16	16.126	chrXVI:15039503	418642494	18	29.831	chrXVIII:13352631	120258546
16	16.894	chrXVI:16058672	252841101	18	31.323	chrXVIII:5765162	120258540
16	19.173	chrXVI:17471373	418642502	18	31.327	chrXVIII:4836241	120258539
16	19.623	chrXVI:18106789	120258529	18	34.367	chrXVIII:3137228	
16	21.464	chrXVI:17895677	244222938	18	41.287	chrXVIII:1211531	418642530
16	22.417	chrXVI:17405918	418642501	19	0	chrXIX:8190806	120258554
16	24.961	chrXVI:17236926	244222936	19	0.054	chrXIX:14650559	418641975
16	31.626	chrXVI:16673569	120258528	19	0.099	chrXIX:18045399	120258558
16	38.499	chrUn:37016121	418642651	19	0.102	CH213.119K16:14070	418641977
16	43.334	chrUn:26389255	244222992	19	0.102	CH213.21C23:188808	418641953
17	0	chrXVII:1733515	418642509	19	0.434	chrXIX:3737235	418641965
17	8.642	chrXVII:12666712	418642526	19	0.554	chrXIX:18043409	252841059
17	10.714	chrXVII:2664810	244222940	19	15.488	chrXIX:1546489	418641958
17	11.707	chrXVII:2626658	418642511	19	16.847	chrXIX:1472847	120258551
17	13.517	chrXVII:2872553	418642512	19	30.53	chrXIX:897343	418641956
17	18.03	chrXVII:3906379	244222942	20	0	chrXX:12622695	244222966
17	18.272	chrXVII:10329401	418642524	20	0	chrXX:12810044	252841048
17	18.272	chrXVII:9697366	244222947	20	0.278	chrXX:14562943	418642569
17	19.473	chrXVII:3843835	120258534	20	0.588	chrXX:14462157	244222968
17	20.238	chrXVII:4909843	244222944	20	0.724	chrXX:14859034	418642571
17	20.598	chrUn:2474754	418642603	20	1.646	chrXX:5734841	418642558
17	20.713	chrUn:2776586	120258568	20	3.948	chrXX:15996390	418642573
17	20.713	chrUn:2632376	252841074	20	8.045	chrXX:16253512	252841060
17	21.65	chrXVII:2999556	418642513	20	16.409	chrXX:2080510	418642553
17	23.546	chrXVII:9881295	418642523	20	22.695	chrUn:30545876	120258573

Linkage Group	Map Position (cM)	Marker name (chromosome: position)	NCBI submitted SNP ID numbers (ss#)	Linkage Group	Map Position (cM)	Marker name (chromosome: position)	NCBI submitted SNP ID numbers (ss#)
21	0	chrUn:31339987	244222998				
21	2.453	chrUn:28158103	418642634				
21	24.879	chrXXI:11060209	120258566				
21	26.406	chrXXI:10969152	244222981				
21	31.416	chrUn:23042966	418642626				
21	40.24	chrXXI:9820534	418642589				
21	42.589	chrXXI:7002178	244222977				
21	42.816	chrXXI:5737465	244222973				
21	44.076	chrXXI:3082227	418642585				
21	44.583	chrUn:6720054	244222987				

Table S3 Paxton Lake QTL scan results

(Starts on next page) The QTL scan results for all QTL detected in our Paxton Lake scan are shown. Together, the '1.5 LOD C.I. low (cM)' and '1.5 LOD C.I. high (cM)' columns indicate the range of the 1.5 LOD confidence interval of the genomic location of the QTL. The 'LOD' column indicates the LOD score at the peak marker for the QTL (the maker at which genotypes showed the strongest association with phenotypes). The 'p-value' column indicates the genome-wide significance of the peak marker's LOD score for the associated trait. When QTL were not included in the 'candidate QTL' dataset, the reason is indicated ("combined scan" means that a co-locating QTL was discovered in the combined scan, which we used instead; "trait not parallel" means that the associated trait was not determined to have diverged in parallel and therefore was not a focus of the study.)

Trait	Linkage group	Peak Marker Position (cM)	1.5 LOD C.I. low (cM)	1.5 LOD C.I. high (cM)	LOD	p-value	Candidate QTL?
plate count	7	33.93	33.41	34.99	16.65	<1.00E-04	no (combined scan)
long gill raker count	3	36	30.9	42	6.43	1.70E-03	no (combined scan)
long gill raker count	7	34.01	32.22	35.81	8.66	<1.00E-04	no (combined scan)
short gill raker count	1	21.16	16	23.72	6.05	3.50E-03	no (combined scan)
short gill raker count	7	34.99	32.22	35.81	5.54	7.60E-03	no (combined scan)
1st dorsal spine	2	33.63	22	39.26	8.11	<1.00E-04	no (trait not parallel)
2nd dorsal spine	20	1.65	0	22.7	4.39	3.68E-02	no (trait not parallel)
x1	1	20	16.42	21.75	5.05	1.86E-02	no (trait not parallel)
y1	8	18.19	10	30	5.12	1.58E-02	no (combined scan)
x2	7	0	0	14	6.38	1.70E-03	yes
x3	1	21.16	16.42	23.72	9.14	<1.00E-04	no (trait not parallel)
x3	5	52	26	56.44	5.65	6.60E-03	no (trait not parallel)
x3	12	13.5	12.16	24	10.23	<1.00E-04	no (trait not parallel)
y3	7	6	0	14	11.12	<1.00E-04	no (combined scan)
x4	3	10	4	16	5.68	5.20E-03	no (trait not parallel)
x4	7	34.21	32.22	35.81	7.61	4.00E-04	no (trait not parallel)
x4	12	20	7.73	25.01	5.09	1.50E-02	no (trait not parallel)
y4	7	34.99	32	37.03	5.27	1.08E-02	no (combined scan)
y5	19	2	0	10	5.11	1.55E-02	yes
x6	7	35.45	30	54	5.61	5.50E-03	no (combined scan)
y6	7	35.45	14.71	40	4.47	4.79E-02	no (trait not parallel)
y6	13	18.72	0	24.53	5.1	1.80E-02	no (trait not parallel)
y6	19	0.1	0	4	11.3	<1.00E-04	no (trait not parallel)
x10	7	40	34.45	50	5.54	7.80E-03	no (trait not parallel)
y10	4	58	35.12	71.36	6.47	1.10E-03	yes
y10	14	11.23	0	22	7.32	2.00E-04	no (combined scan)
x11	1	21.16	16.42	23.72	5.94	3.90E-03	no (trait not parallel)
y11	1	21.75	16.42	23.72	6.82	9.00E-04	no (combined scan)
y11	4	30	26.83	71.36	8.11	3.00E-04	no (combined scan)
x12	1	19.11	16	23.72	4.71	2.95E-02	no (trait not parallel)
y12	4	28.15	26	71.36	4.62	3.74E-02	yes
y12	19	0.1	0	8	5.13	1.59E-02	no (combined scan)
x13	1	19.11	16.42	27.92	7.15	3.00E-04	no (combined scan)
x13	7	35.12	24	40	4.58	4.24E-02	no (combined scan)
x16	1	19.11	16.42	27.92	4.76	2.85E-02	no (combined scan)
x16	13	20.04	8.48	27.7	4.44	4.93E-02	yes
x18	7	32.22	26.61	33.93	4.84	2.52E-02	no (combined scan)
y18	4	36	30.31	71.36	4.53	4.11E-02	yes
x19	10	8	6.2	24	4.96	2.00E-02	no (trait not parallel)
y19	8	26	19.01	30.86	6.83	1.00E-03	no (trait not parallel)
y19	12	12.16	10	25.01	4.84	2.73E-02	no (trait not parallel)
x20	1	25.31	24	34	4.36	5.30E-02	yes

Trait	Linkage group	Peak Marker Position (cM)	1.5 LOD C.I. low (cM)	1.5 LOD C.I. high (cM)	LOD	p-value	Candidate QTL?
x21	1	20	16.42	22.4	4.9	2.32E-02	yes
x22	7	33.93	24	35.45	4.62	4.06E-02	yes
x23	1	19.11	16.42	27.92	8.51	<1.00E-04	no (trait not parallel)
x24	1	19.11	16	26	5.62	6.40E-03	no (trait not parallel)
x25	1	20	16	26	4.53	4.33E-02	no (trait not parallel)
x25	16	12.99	0	24	4.48	4.74E-02	no (trait not parallel)
y25	12	18	12.16	25.01	7.67	<1.00E-04	no (combined scan)
x26	1	19.11	16	26	5.13	1.47E-02	no (trait not parallel)
y26	19	0.1	0	6	4.85	2.63E-02	no (combined scan)
centroid	19	0.1	0	6	4.67	3.42E-02	yes

Table S4 Priest Lake QTL scan results

(Starts on next page) The QTL scan results for all QTL detected in our Priest Lake scan are shown. Together, the '1.5 LOD C.I. low (cM)' and '1.5 LOD C.I. high (cM)' columns indicate the range of the 1.5 LOD confidence interval of the genomic location of the QTL. The 'LOD' column indicates the LOD score at the peak marker for the QTL (the maker at which genotypes showed the strongest association with phenotypes). The 'p-value' column indicates the genome-wide significance of the peak marker's LOD score for the associated trait. When QTL were not included in the 'candidate QTL' dataset, the reason is indicated ("combined scan" means that a co-locating QTL was discovered in the combined scan, which we used instead; "trait not parallel" means that the associated trait was not determined to have diverged in parallel and therefore was not a focus of the study.)

Trait	Linkage group	Peak Marker Position (cM)	1.5 LOD C.I. low (cM)	1.5 LOD C.I. high (cM)	LOD	p-value	Candidate QTL?
plate count	2	26	18	44	4.41	2.34E-02	no (combined scan)
plate count	7	35.45	30	42	8.58	<1.00E-04	no (combined scan)
plate count	16	14	6.33	22	5.5	2.70E-03	no (combined scan)
long gill raker count	7	46	32.22	58	6.13	1.70E-03	no (combined scan)
short gill raker count	1	14.83	6	32	4.67	1.69E-02	no (combined scan)
x1	2	24	18	33.63	9.52	<1.00E-04	no (trait not parallel)
x2	14	38.82	30.98	48.93	4.04	4.88E-02	yes
x3	14	38.82	28.55	48.93	4.38	2.47E-02	no (trait not parallel)
y3	4	71.36	66	71.36	4.67	1.51E-02	no (combined scan)
y5	7	40	34.21	56	6.16	1.40E-03	no (combined scan)
x6	4	20.84	14.49	32	3.99	5.35E-02	yes
x6	13	27.7	22.18	28.79	4.06	4.64E-02	yes
x7	3	6	0	14	5.32	4.80E-03	no (trait not parallel)
y7	7	35.45	30	50.64	5.58	3.50E-03	no (combined scan)
y7	9	10	0	17.66	4.32	2.97E-02	yes
y10	1	23.96	4	27.92	5.8	1.80E-03	no (combined scan)
y11	11	30	8.46	37.74	4.86	8.30E-03	no (combined scan)
x15	3	2.69	0	12	4.2	3.39E-02	no (trait not parallel)
x16	1	21.75	18.11	34	5.4	3.20E-03	no (combined scan)
x16	12	13.5	2	15.46	5.68	1.70E-03	no (combined scan)
y16	21	42.82	26	44.58	4.19	4.17E-02	yes
x17	12	6.42	4	13.24	6.31	7.00E-04	no (combined scan)
x17	14	34.83	24	48.93	4.1	4.36E-02	yes
y18	11	34.66	28	40	4.31	3.04E-02	no (combined scan)
y19	1	22	16	37.75	5.87	9.00E-04	no (trait not parallel)
y19	12	12.16	0	24	4.3	3.20E-02	no (trait not parallel)
y19	14	34.83	0	41.41	4.53	2.15E-02	no (trait not parallel)
x20	12	4.39	0	15.46	4.56	1.86E-02	yes
x23	3	4	0	12	4.69	1.54E-02	no (trait not parallel)
y23	21	44	20	44.58	5.35	4.70E-03	no (trait not parallel)
y25	12	11.57	9.45	15.46	4.09	4.82E-02	no (combined scan)
y26	1	21.75	18.11	30	7.02	<1.00E-04	no (combined scan)
y26	12	15.46	3.74	25.01	4.7	1.42E-02	no (combined scan)
y26	14	36.5	12	48.93	4.13	3.94E-02	yes
y27	12	4.39	0	15.46	4.47	2.19E-02	no (combined scan)
y27	17	21.65	0	27.82	4.29	2.99E-02	no (combined scan)
centroid	1	24.57	22.4	32	6.74	3.00E-04	no (combined scan)

Table S5 'Combined' QTL scan results

(Starts on next page) The QTL scan results for all QTL detected in our 'combined scan' (i.e. Paxton and Priest Lakes, and including a genotype by lake interaction covariate) are shown. Together, the '1.5 LOD C.I. low (cM)' and '1.5 LOD C.I. high (cM)' columns indicate the range of the 1.5 LOD confidence interval of the genomic location of the QTL. The 'LOD' column indicates the LOD score at the peak marker for the QTL (the maker at which genotypes showed the strongest association with phenotypes). The 'p-value' column indicates the genome-wide significance of the peak marker's LOD score for the associated trait. When QTL were not included in the 'candidate QTL' dataset, the reason is indicated ("trait not parallel" means that the associated trait was not determined to have diverged in parallel and therefore was not a focus of the study.)

Trait	Linkage group	Peak Marker Position (cM)	1.5 LOD C.I. low (cM)	1.5 LOD C.I. high (cM)	LOD	p-value	Candidate QTL?
plate count	2	24	18	39.1	5.59	5.27E-02	yes
plate count	7	33.93	33.41	34.99	24.81	<1.00E-04	yes
plate count	16	9.98	4	22	5.66	4.68E-02	yes
long gill raker count	3	36	30.9	42	7.29	2.30E-03	yes
long gill raker count	7	35.12	33.41	35.81	14.12	<1.00E-04	yes
short gill raker count	1	21.16	14	23.72	9.43	2.00E-04	yes
short gill raker count	7	34.99	32.22	35.81	6.67	9.40E-03	yes
1st dorsal spine	2	33.63	24	39.26	10.39	<1.00E-04	no (trait not parallel)
x1	2	26	18	33.05	10.61	<1.00E-04	no (trait not parallel)
y1	8	18	10	30.86	5.97	3.45E-02	yes
x2	4	23.78	14.49	26.83	5.97	5.01E-02	yes
x3	1	21.16	16.42	22.4	8.16	1.40E-03	no (trait not parallel)
x3	5	50.52	30	56.44	6.4	1.57E-02	no (trait not parallel)
x3	12	18	8	25.01	8.57	6.00E-04	no (trait not parallel)
y3	4	71.36	66	71.36	5.8	4.04E-02	yes
y3	7	6	0	14	10.65	<1.00E-04	yes
x4	7	33.93	26.61	35.81	8.4	1.10E-03	no (trait not parallel)
y4	7	34.99	32.22	37.03	5.81	4.95E-02	yes
y5	7	35.45	34.21	42	9.77	<1.00E-04	yes
x6	7	34.21	30	50.99	6.18	1.92E-02	yes
y6	7	37.32	26.61	44	6.86	6.80E-03	no (trait not parallel)
y6	13	12	0	23.99	7.32	2.80E-03	no (trait not parallel)
y6	19	0	0	4	11.42	<1.00E-04	no (trait not parallel)
x7	3	6	0.22	12	7.61	1.70E-03	no (trait not parallel)
y7	2	33.63	30	38	6.05	2.52E-02	yes
y7	7	35.45	32.22	56	6.41	1.36E-02	yes
x9	3	4	0	10	5.89	3.10E-02	no (trait not parallel)
x10	2	36.63	28	42	5.71	4.66E-02	no (trait not parallel)
y10	1	19.11	18.11	26	8.36	5.00E-04	yes
y10	14	12	0	22	10.43	<1.00E-04	yes
x11	1	21.16	16.42	23.72	5.96	3.77E-02	no (trait not parallel)
y11	1	21.16	15.32	26	5.86	5.35E-02	yes
y11	4	30	26.83	71.36	6.31	2.86E-02	yes
y11	11	28	10	37.74	6.7	1.58E-02	yes
x12	19	0.55	0	6	6.12	4.57E-02	no (trait not parallel)
y12	13	27.7	24.53	28.79	6	4.21E-02	yes
y12	19	0	0	10	6.85	1.28E-02	yes
x13	1	18.11	16	30	6.51	2.34E-02	yes
x13	7	28	24	33.41	6.87	1.37E-02	yes
x16	1	21.75	18.11	23.72	9.67	<1.00E-04	yes
x16	12	5.22	2	15.46	6.92	5.60E-03	yes
y16	13	28.79	24	28.79	6.18	2.02E-02	yes

Trait	Linkage group	Peak Marker Position (cM)	1.5 LOD C.I. low (cM)	1.5 LOD C.I. high (cM)	LOD	p-value	Candidate QTL?
x17	12	6.42	4	15.46	6.87	9.50E-03	yes
x18	7	32.22	29.3	37.03	6.51	1.12E-02	yes
y18	11	34	28	42	6.44	1.24E-02	yes
y19	1	21.75	14	41.89	6.25	2.17E-02	no (trait not parallel)
y19	4	34.54	30.31	38	6.7	1.02E-02	no (trait not parallel)
y19	8	26	19.01	30.86	6.97	6.50E-03	no (trait not parallel)
y19	12	12.16	10.86	15.46	9.25	1.00E-04	no (trait not parallel)
y19	14	11.23	0	36	6.01	3.22E-02	no (trait not parallel)
y19	19	0	0	6	6.19	2.46E-02	no (trait not parallel)
x20	4	20	15.02	23.78	6.42	1.28E-02	yes
y22	1	18	15.32	20.27	6.71	9.20E-03	no (trait not parallel)
x23	1	21.16	16.42	23.72	6.75	1.67E-02	no (trait not parallel)
x23	3	6	0	10.46	8.19	2.00E-03	no (trait not parallel)
y25	12	13.24	10.86	21	11.06	<1.00E-04	yes
y26	1	21.75	18.11	34	7.91	9.00E-04	yes
y26	12	13.24	10.86	22	9.37	<1.00E-04	yes
y26	19	0.55	0	6	6.83	9.00E-03	yes
y27	8	19.01	16.61	30.86	5.54	5.42E-02	yes
y27	12	13.24	10.73	24	7.51	2.90E-03	yes
y27	17	21.65	12	27.82	7.15	4.40E-03	yes
centroid	1	24.57	2	32	9.64	3.00E-04	yes

Table S6 QTL effects of candidate QTL

(Starts on next page) QTL effect was considered 'parallel' when either the best model of the QTL effect was 'same effect', or when the best model of QTL effect was 'different effect' but the direction of additive effects were 'same'. QTL effect was considered only in a 'single lake' when the best model of the QTL effect was either 'effect in Paxton only' or 'effect in Priest only'. QTL effect was considered 'opposite' when the best model of QTL effect was 'different effect' and the direction of additive effects were 'opposite'. The second best model of QTL effect and the delta AICc between it and the best model is also shown. When the delta AICc was less than two and the 2nd best model called for a different QTL effect category than the best model did, we dropped the QTL from any analysis in which QTL effect category was a variable study (indicated by 'NA' in the ''QTL effect' based on AICc model selection' column). PVE for each QTL in each lake was determined using 'single QTL, single lake linear models'. The 'Priest Entropy' and 'Paxton Entropy' columns show the entropy values (an index of genotype information content, where lower values indicate greater information content), in each lake's cross at the QTL's peak marker.

Trait	Scan QTL was detected in	Linkage group	Peak Marker Position (cM)	Direction of additive effects	'QTL Effect' based on AICc model selection	Best model of QTL effect	2nd best model of QTL effect	Delta AICc	PVE in Priest	PVE in Paxton	Priest entropy	Paxton entropy
plate count	combined	2	24	same	Parallel	same effect	different effect	2.21	4.9	1.32	0.28	0.27
plate count	combined	7	33.93	same	Parallel	different effect	same effect	0.94	9.1	12.09	0.04	0.03
plate count	combined	16	9.98	opposite	Opposite	different effect	effect in Priest only	2.03	6.06	0.73	0.06	0.17
long gill raker count	combined	7	35.12	same	Parallel	same effect	different effect	2.26	6.51	6.3	0.01	0.08
long gill raker count	combined	3	36	same	NA	effect in Paxton only	different effect	1.12	1.08	5	0.14	0.14
short gill raker count	combined	1	21.16	same	Parallel	same effect	different effect	2.72	4.13	4.32	0.07	0.17
short gill raker count	combined	7	34.99	same	Parallel	same effect	different effect	0.68	1.67	3.97	0	0.08
y1	combined	8	18	same	Single lake	effect in Paxton only	same effect	4.14	1.58	4.18	0.09	0.12
x2	combined	4	23.78	same	Parallel	same effect	different effect	2.99	1.48	1.13	0.08	0.21
x2	Paxton	7	0	same	NA	effect in Paxton only	same effect	0.58	0.07	2.39	0.71	0.05
x2	Priest	14	38.82	opposite	NA	effect in Priest only	different effect	0.39	1.92	0.37	0.08	0.16
y3	combined	4	71.36	opposite	NA	different effect	effect in Priest only	1.38	5.29	0.9	0.06	0.88
y3	combined	7	6	opposite	Single lake	effect in Paxton only	different effect	2.49	0.13	8.86	0.5	0.13
y4	combined	7	34.99	same	Parallel	same effect	different effect	2	1.56	4.08	0	0.08
y5	combined	7	35.45	same	Parallel	same effect	different effect	2.42	4.34	2.51	0	0.12
y5	Paxton	19	2	same	Parallel	same effect	different effect	0.42	0.21	3.63	0.19	0.05
x6	combined	7	34.21	opposite	NA	different effect	effect in Paxton only	0.92	0.68	3.4	0.02	0.05
x6	Priest	4	20.84	same	Parallel	same effect	different effect	1.81	3.09	0.7	0.05	0.2
x6	Priest	13	27.7	same	Single lake	effect in Priest only	same effect	7.08	3.15	0.08	0.1	0.2
y7	combined	7	35.45	same	NA	effect in Priest only	different effect	0.94	5.9	0.52	0	0.12
y7	combined	2	33.63	opposite	Opposite	different effect	effect in Paxton only	5.61	2.41	3.14	0.03	0.04
y7	Priest	9	10	same	Single lake	effect in Priest only	same effect	3.44	4.61	0.59	0.35	0.34
y10	combined	1	19.11	opposite	Opposite	different effect	effect in Priest only	9.03	2.77	1.63	0	0.01
y10	combined	14	12	same	Parallel	same effect	different effect	0.31	1.23	4.22	0.06	0.2
y10	Paxton	4	58	opposite	Single lake	effect in Paxton only	different effect	2.57	0.09	3.76	0.03	0.74
y11	combined	11	28	same	NA	effect in Priest only	different effect	0.57	2.45	0.37	0.13	0.12
y11	combined	1	21.16	opposite	Single lake	effect in Paxton only	different effect	5.1	0.35	3.49	0.07	0.17
y11	combined	4	30	same	Single lake	effect in Paxton only	different effect	2.4	0.38	4.13	0.01	0.24
y12	combined	19	0	same	Single lake	effect in Priest only	different effect	13.99	2.03	3.11	0.22	0.03
y12	combined	13	27.7	same	Parallel	same effect	different effect	3.01	1.96	1.58	0.1	0.2
y12	Paxton	4	28.15	same	Single lake	effect in Paxton only	different effect	2.77	0.55	2.81	0.06	0.19
x13	combined	7	28	opposite	NA	same effect	different effect	0.23	2.3	1.91	0.09	0.22

Trait	Scan QTL was detected in	Linkage group	Peak Marker Position (cM)	Direction of additive effects	'QTL Effect' based on AICc model selection	Best model of QTL effect	2nd best model of QTL effect	Delta AICc	PVE in Priest	PVE in Paxton	Priest entropy	Paxton entropy
x13	combined	1	18.11	same	Parallel	same effect	different effect	0.31	0.57	3.71	0.08	0.17
x16	combined	1	21.75	same	Parallel	same effect	different effect	2.97	6.19	3.32	0.11	0.2
x16	combined	12	5.22	same	Parallel	different effect	same effect	0.87	5.45	1.36	0.06	0.16
x16	Paxton	13	20.04	same	Parallel	different effect	same effect	1.02	0.98	3.39	0.05	0.07
y16	combined	13	28.79	opposite	NA	different effect	same effect	0.83	3.55	2.08	0.16	0.26
y16	Priest	21	42.82	same	NA	same effect	effect in Priest only	0.34	4.22	0.54	0.01	0.87
x17	combined	12	6.42	opposite	Single lake	effect in Priest only	different effect	3.69	6.84	0.01	0.16	0.22
x17	Priest	14	34.83	same	Single lake	effect in Priest only	different effect	2.58	4.52	0.29	0	0.22
x18	combined	7	32.22	opposite	Single lake	effect in Paxton only	different effect	4.02	2.06	3.84	0.06	0.11
y18	combined	11	34	same	Parallel	same effect	different effect	1.45	2.71	1.27	0.03	0.03
y18	Paxton	4	36	opposite	Single lake	effect in Paxton only	different effect	9.02	0.16	2.85	0.02	0.04
x20	combined	4	20	opposite	Single lake	effect in Priest only	effect in Paxton only	3.16	3.58	2.15	0.04	0.19
x20	Paxton	1	25.31	same	NA	different effect	effect in Paxton only	1.62	1.18	3.32	0.13	0.15
x20	Priest	12	4.39	opposite	NA	different effect	effect in Priest only	1.21	4.34	0.75	0.05	0.17
x21	Paxton	1	20	same	Single lake	effect in Paxton only	same effect	2.57	0.25	2.51	0.01	0.01
x22	Paxton	7	33.93	same	NA	different effect	effect in Paxton only	0.06	0.73	3.94	0.04	0.03
y25	combined	12	13.24	same	Parallel	same effect	different effect	2.88	4.71	5.64	0.02	0.04
y26	combined	1	21.75	opposite	Single lake	effect in Priest only	different effect	2.66	4.71	0.07	0.11	0.2
y26	combined	12	13.24	same	Parallel	same effect	different effect	2.36	3.17	2.57	0.02	0.04
y26	combined	19	0.55	same	Parallel	different effect	effect in Priest only	5.04	1.18	2.79	0.19	0.04
y26	Priest	14	36.5	opposite	Single lake	effect in Priest only	different effect	6.62	2.83	0.05	0.07	0.18
y27	combined	12	13.24	same	Parallel	same effect	different effect	2.55	4.16	2.91	0.02	0.04
y27	combined	17	21.65	opposite	Opposite	different effect	effect in Priest only	10.7	4.81	2.95	0.11	0.1
y27	combined	8	19.01	same	Single lake	effect in Paxton only	effect in Priest only	1.4	2.76	2.53	0.01	0.1
centroid	combined	1	24.57	same	NA	effect in Priest only	different effect	1.14	6.4	0.91	0.07	0.13
centroid	Paxton	19	0.1	opposite	NA	effect in Priest only	same effect	1.28	1.24	2.96	0.21	0.02

Table S7 Principal components of parallel traits

32 principal components of 32 parallel traits in Paxton and Priest Lake F_2 individuals. Classification of the species divergence of each principal component (based on model selection technique described in the 'Identifying parallel phenotypic evolution' subsection of the Methods) as parallel, single lake, opposite or not able to be classified (–) is shown under 'PC divergence category'. The number of QTL detected for parallel principal components is also shown. For the effect categories of QTL that underlie parallel principal components that explain up to 90 percent of the cumulative variance, refer to Figure S5.

Principal component	Standard deviation	Percent of variance	Cumulative percent of variance	PC divergence category	Number of QTL detected
Comp.1	2.516	19.8	19.8	Parallel	1
Comp.2	1.939	11.7	31.5	Parallel	0
Comp.3	1.601	8.0	39.5	Parallel	2
Comp.4	1.502	7.0	46.6	Parallel	5
Comp.5	1.303	5.3	51.9	Parallel	1
Comp.6	1.223	4.7	56.6	–	–
Comp.7	1.185	4.4	60.9	Parallel	4
Comp.8	1.125	4.0	64.9	Parallel	3
Comp.9	1.053	3.5	68.4	Parallel	3
Comp.10	0.998	3.1	71.5	Single lake	–
Comp.11	0.992	3.1	74.5	–	–
Comp.12	0.907	2.6	77.1	Parallel	2
Comp.13	0.869	2.4	79.5	–	–
Comp.14	0.849	2.2	81.7	Parallel	0
Comp.15	0.839	2.2	83.9	Parallel	1
Comp.16	0.799	2.0	85.9	Parallel	1
Comp.17	0.745	1.7	87.7	Parallel	0
Comp.18	0.718	1.6	89.3	–	–
Comp.19	0.658	1.4	90.6	Parallel	0
Comp.20	0.639	1.3	91.9	Opposite	–
Comp.21	0.619	1.2	93.1	Parallel	2
Comp.22	0.574	1.0	94.1	–	–
Comp.23	0.543	0.9	95.0	–	–
Comp.24	0.534	0.9	95.9	Single lake	–
Comp.25	0.516	0.8	96.8	Parallel	0
Comp.26	0.474	0.7	97.5	–	–
Comp.27	0.432	0.6	98.0	–	–
Comp.28	0.407	0.5	98.6	–	–
Comp.29	0.388	0.5	99.0	–	–
Comp.30	0.373	0.4	99.5	–	–
Comp.31	0.337	0.4	99.8	Parallel	0
Comp.32	0.235	0.2	100.0	Single lake	–

Table S8 Proportional similarity of QTL use underlying parallel traits

(Starts on next page) For each QTL, 'PVE in Priest' and 'PVE in Paxton' were determined using a 'multiple QTL linear model' containing genotypic effects of each QTL affecting the same trait (as well as family identity and sex as covariates). These models were run for each lake separately. If the QTL genotype (both additive and dominant components) did not show a significant effect when dropped from a 'single lake, single QTL linear model' then it was not entered in the multiple QTL model for that lake. In this case, the PVE column is left blank. In each lake, proportional contributions of QTL to traits were calculated by scaling the PVEs of all QTL affecting the same trait so that they summed to 1. The proportional similarity of a QTL was taken as the overlap in the proportional contributions of that QTL in the two lakes. The 'proportional similarity of QTL use' underlying any given trait is then the sum of the proportional similarities of all QTL affecting that trait.

Trait	QTL (LG # @ position (cM))	PVE in Priest	Proportional Contribution in Priest	PVE in Paxton	Proportional Contribution in Paxton	Proportional Similarity
plate count	16@10.0	4.79	0.31			0.00
plate count	2@24.0	3.39	0.22	1.28	0.10	0.10
plate count	7@33.9	7.32	0.47	12.04	0.90	0.47
long gill raker count	7@35.1	6.51	1.00	6.23	0.56	0.56
long gill raker count	3@36.0			4.93	0.44	0.00
short gill raker count	1@21.2	4.13	1.00	4.89	0.52	0.52
short gill raker count	7@35.0			4.54	0.48	0.00
y1	8@18.0	1.58	1.00	4.18	1.00	1.00
x2	14@38.8	1.70	0.57			0.00
x2	4@23.8	1.26	0.43	1.11	0.32	0.32
x2	7@0.0			2.38	0.68	0.00
y3	4@71.4	5.29	1.00			0.00
y3	7@6.0			8.86	1.00	0.00
y4	7@35.0			4.08	1.00	0.00
y5	7@35.5	4.34	1.00	2.44	0.41	0.41
y5	19@2.0			3.57	0.59	0.00
x6	13@27.7	3.11	0.50			0.00
x6	4@20.8	3.06	0.50			0.00
x6	7@34.2			3.40	1.00	0.00
y7	2@33.6	1.43	0.12	3.14	1.00	0.12
y7	7@35.5	5.98	0.49			0.00
y7	9@10.0	4.74	0.39			0.00
y10	1@19.1	2.61	0.71	0.73	0.11	0.11
y10	14@12.0	1.07	0.29	3.51	0.51	0.29
y10	4@58.0			2.68	0.39	0.00
y11	11@28.0	2.45	1.00			0.00
y11	1@21.2			2.60	0.44	0.00
y11	4@30.0			3.24	0.56	0.00
y12	13@27.7	1.54	0.49	1.35	0.19	0.19
y12	19@0.0	1.61	0.51	3.14	0.44	0.44
y12	4@28.1			2.69	0.37	0.00
x13	7@28.0	2.30	1.00	1.31	0.30	0.30
x13	1@18.1			3.11	0.70	0.00
x16	1@21.7	4.53	0.54	2.31	0.37	0.37
x16	12@5.2	3.79	0.46	1.16	0.18	0.18
x16	13@20.0			2.83	0.45	0.00
y16	13@28.8	3.03	0.45	2.08	1.00	0.45
y16	21@42.8	3.70	0.55			0.00
x17	12@6.4	6.00	0.62			0.00

Trait	QTL (LG # @ position (cM))	PVE in Priest	Proportional Contribution in Priest	PVE in Paxton	Proportional Contribution in Paxton	Proportional Similarity
x17	14@34.8	3.68	0.38			0.00
x18	7@32.2	2.06	1.00	3.84	1.00	1.00
y18	11@34.0	2.71	1.00	0.88	0.26	0.26
y18	4@36.0			2.47	0.74	0.00
x20	12@4.4	4.15	0.55			0.00
x20	4@20.0	3.40	0.45	1.61	0.37	0.37
x20	1@25.3			2.78	0.63	0.00
x21	1@20.0			2.51	1.00	0.00
x22	7@33.9			3.94	1.00	0.00
y25	12@13.2	4.71	1.00	5.64	1.00	1.00
y26	1@21.7	3.02	0.38			0.00
y26	12@13.2	2.07	0.26	3.00	0.48	0.26
y26	14@36.5	1.62	0.20			0.00
y26	19@0.6	1.21	0.15	3.22	0.52	0.15
y27	12@13.2	3.47	0.34	2.87	0.35	0.34
y27	17@21.7	4.36	0.43	3.17	0.38	0.38
y27	8@19.0	2.36	0.23	2.21	0.27	0.23
centroid size	1@24.6	6.40	1.00			0.00
centroid size	19@0.1			2.96	1.00	0.00

References

Arnegard, M. E., M. D. McGee, B. Matthews, K. B. Marchinko, G. L. Conte, et al., 2014 Genetics of ecological divergence during speciation. Nature 511: 307–311.

Jones, F. C., M. G. Grabherr, Y. F. Chan, P. Russell, E. Mauceli, et al., 2012 The genomic basis of adaptive evolution in threespine sticklebacks. Nature 484: 55–61.